

A stochastic individual-based model for immunotherapy of cancer

Martina Baar*, Loren Coquille*, Hannah Mayer*,
Michael Hölzel, Meri Rogava, Thomas Tüting,
Anton Bovier

Version of July 19, 2022

Abstract We propose an extension of a standard stochastic individual-based model in population dynamics which broadens the range of biological applications. Our primary motivation is modelling of immunotherapy for malignant tumors. The main characteristics of the model are distinguishing phenotype and genotype, including environment-dependent transitions between phenotypes that do not affect the genotype, and the introduction of a competition term which lowers the reproduction rate of an individual in addition to the usual term that increases its death rate. We prove that this stochastic process converges in the limit of large populations to a deterministic limit which is the solution to a system of quadratic differential equations. We illustrate the new setup by using it to model various phenomena arising in immunotherapy. Our aim is twofold: on the one hand, we show that the interplay of genetic mutations and phenotypic switches on different timescales as well as the occurrence of metastability phenomena raise new mathematical challenges. On the other hand, we argue why understanding purely stochastic events (which cannot be obtained with deterministic systems) may help to understand the resistance of tumors to various therapeutic approaches and may have non-trivial consequences on tumor treatment protocols and demonstrate this through numerical simulations.

Keywords adaptive dynamics, stochastic individual-based models, cancer, immunotherapy

Mathematics Subject Classification (2000) 60K35,92D25,60J85

Acknowledgements We acknowledge financial support from the German Research Foundation (DFG) through the *Hausdorff Center for Mathematics*, the Cluster of Excellence *ImmunoSensation*, the Priority Programme SPP1590 *Probabilistic Structures in Evolution*, and the Collaborative Research Centre 1060 *The Mathematics of Emergent Effects*. We thank Boris Prochnau for programming.

* Equal contributions

M. Baar, L. Coquille, H. Mayer, A. Bovier
Institute for Applied Mathematics, Bonn University, Endenicher Allee 60, 53115 Bonn, Germany.
E-mail: mbaar@uni-bonn.de, lcoquill@uni-bonn.de, hannah.mayer@uni-bonn.de, bovier@uni-bonn.de

M. Hölzel
Institute for Clinical Chemistry and Clinical Pharmacology, University Hospital, Bonn University, Sigmund-Freud
Strasse 25, 53127 Bonn, Germany.
E-mail: michael.hoelzel@ukb.uni-bonn.de

M. Rogava, T. Tüting
Laboratory of Experimental Dermatology, Department of Dermatology and Allergy, University Hospital, Bonn
University, Sigmund-Freud-Strasse 25, 53127 Bonn, Germany.
E-mail: meri.rogava@ukb.uni-bonn.de, thomas.tueting@ukb.uni-bonn.de

Contents

1	Introduction	2
1.1	Biological motivation and background information	2
1.2	Scaling limits in models of adaptive dynamics	4
1.3	Outline of the objective of the model	5
2	The model	6
2.1	General notations	6
2.2	The dynamics	7
2.3	Simulation	10
3	Convergence result	10
4	Key examples	11
4.1	Different relapse behaviour due to random fluctuations	11
4.1.1	Therapy with T-cells with one specificity	11
4.1.2	Therapy with T-cells with two different specificities	13
4.2	Arrival of a mutant.	17
4.3	The effect of birth-reducing competition on mutation events	21
5	Prediction of the efficacy of immunotherapeutic methods	23
5.1	Therapy with T-cells of one or two specificities with biologically reasonable parameters	23
5.2	Initial values	26
5.3	Therapy-induced early mutation	26

1 Introduction

1.1 Biological motivation and background information

The treatment of various cancers with immunotherapies received a lot of attention in the medical as well as the mathematical modelling communities during the last decades [24,23,20,29,16]. Many different therapy approaches were developed and tested experimentally. For the classical therapies such as surgery, chemotherapy and radiation, but also for immunotherapies, resistance is an issue: although a therapy leads to an initial phase of remission, some kind of resistance is very often acquired and a relapse occurs. The main driving forces for resistance are considered to be the genotypic and phenotypic heterogeneity of tumors, which may be enhanced during therapy, see the review by Hölzel, Bovier and Tüting [24] or [31,20] and references therein. The strong influence of the tumor microenvironment is for example pointed out in [13]. The tumor is to be seen as a complex tissue which evolves in mutual influence with its environment. It can remain for some time in metastable niches but internal or external perturbations can change the behaviour of the whole system.

In this article, we consider the example of melanoma (tumors associated with skin cancer) under T-cell therapy. Our work is motivated by experiments of Landsberg et al. [30], where melanoma in mice under treatment with *adoptive cell transfer* (ACT) therapy are investigated experimentally. For this therapeutic approach certain T-cells (immune cells which are able to kill a specific type of melanomas) are injected into mice bearing melanoma. It is reported in [30] that during such a treatment, a significant problem occurs: the injection of T-cells induces an inflammation and the melanoma cells react to this environmental change by switching their phenotype. The cells pass from a so-called differentiated phenotype to a dedifferentiated one (special markers on the cell surface disappear). More precisely, the phenotype switch occurs if proinflammatory cytokines, called TNF- α (Tumor Necrosis Factor), are present. Since the T-cells recognise the cancerous cells exactly by these markers that are then down-regulated, they are not capable of killing the dedifferentiated cancer cells, and a relapse is often observed. A second reason for the appearance of a relapse is that the T-cells become exhausted and are not working efficiently any more. This problem was addressed by restimulation of the T-cells, but this led only to delay in the occurrence of the relapse.

It was shown in [30] that cell division is not required for switching. The switch is thus a purely phenotypic change which is not induced by a genotypic change like a mutation. In addition, Landsberg *et al.* observed [30] that the switch is reversible, i.e. the melanoma cells can recover their initial (differentiated) phenotype. The final state of the tumor is a mixture of differentiated

and dedifferentiated cells, observed in different proportions for different individuals. Finally, the authors suggest to inject two different types of T-cells in next ACT protocols (one specific to differentiated cells as above, and the other specific to dedifferentiated cells) in order to avoid relapses. We aim at finding a model that can represent the phenomena that were seen in the experiments and with which we can simulate different therapy protocols including protocols where 2 T-cell types are used. This could help finding effective therapy protocols.

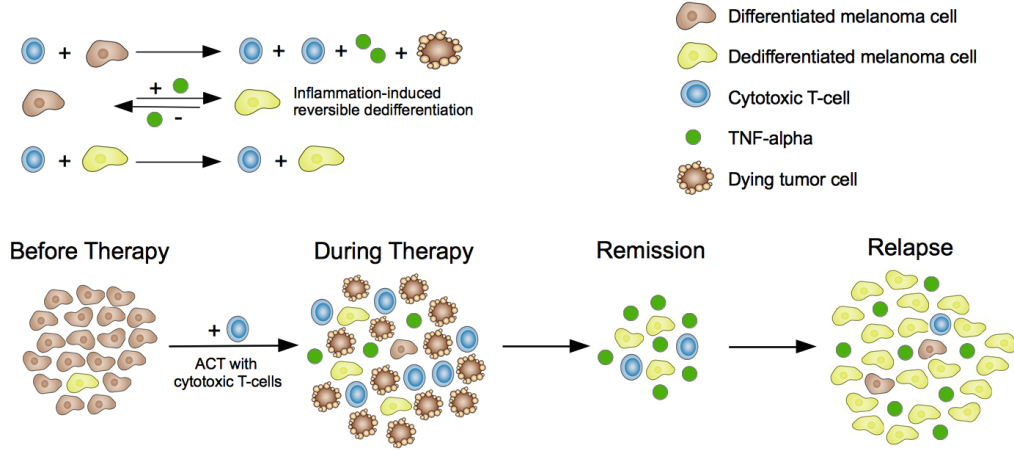


Fig. 1: Schema of therapy by adoptive cell transfer (ACT).

Remark 1 Of course, other immune cells and cytokines are also present in the mouse models. However, according to the careful control experiments carried out by Landsberg et al [30], their influence on the mechanism is negligible. Therefore we focus on the occurrence and influence of the phenotypic switch and our model includes the mechanisms explained above and contains three types of actors: Melanoma cells, T-cells and TNF- α . This is shown schematically in Figure 1 which is adapted from [24].

In order to find better therapy protocols it is very important to understand the mechanisms of resistance and the interplay between therapy and resistance. Mathematical models may help understanding this interplay and could be used to try to predict successful therapy protocols. A number of (mostly deterministic) models have been proposed that aim at describing the development of a tumor under treatment, focussing on different aspects. The case of therapy by adoptive transfer of cells is treated with deterministic models for example in [16]. Let us emphasize that the deterministic models describe the evolution of densities of cells and are considered to be a good approximation of the system when the number of involved cells is large. This neglects effects that involve small numbers of particular cells, where intrinsically random effects have a significant impact. To capture such effects it is necessary to use *stochastic models* that model the individual events of cell births and deaths of cells as random events. While such models converge to the deterministic limits when population sizes scale to infinity, they are able to retain information on important stochastic effects which emerge on longer time-scales or because certain cell-populations are small in some situations. For example, as we will demonstrate later, in the remission phase of a tumor, the influence of random fluctuations can be high, since the tumor and the T-cell populations drop to a low level. Then T-cells may die out due to random fluctuations, an effect that could not be seen in a deterministic model.

To our knowledge the so far developed stochastic models do not describe the coevolution of the tumor cells and immune cells populations. Nevertheless, stochastic approaches are used to understand certain aspects of tumor development, as for example rate models [22] or multi-type branching processes [7, 1].

In this paper, we adapt the stochastic individual-based approach to model *adaptive dynamics* as initiated by Metz et. al [32] and developed in recent years by many authors (see e.g. Bolker and Pacala [4], Diekmann and Law [15], and Champagnat et al. [10,10]), where birth, death, mutation, or switch events of single actors occur at random times, to the setting of tumor growth under immunotherapy described above. We exhibit the existence of intrinsically stochastic phenomena, such as metastability, which may have potentially non-trivial consequences on tumor treatment protocols. We propose the setting of adaptive dynamics as an attractive intermediate modelling framework that allows to capture the system in a quantitatively reasonable way.

1.2 Scaling limits in models of adaptive dynamics

Adaptive population dynamics consists in describing the evolution of populations in the space of phenotypes or geographical locations. The main factors to be modeled are survival fitness, mutations and migrations.

The interaction between individuals is modelled as competition for ecological resources. The goal is to explain how a population spreads, diversifies, and structures itself. Individual-based models describe the dynamics at the level of the individual (birth, death, reproduction, and aim at deriving the predictions of adaptive dynamics for the overall dynamics of the population.

One of the standard models, called BPDFL after publications of Bolker, Pacala, Diekmann and Law [4,5,15], is a Markov process on a space of point measures. The space \mathcal{X} of traits or types of individuals (e.g. $\mathbb{R}^d, \mathbb{Z}^d$) represents some properties of individuals (height, size of a leg, etc.) and the configuration space is the space of point measures $\nu_t = \sum_{i=1}^{N_t} \delta_{x_i(t)}$ on \mathcal{X} , representing a population of N_t individuals at time t . The individual i carries trait $x_i(t) \in \mathcal{X}$. The dynamics for each individual are characterised by parameters attached to the trait. Each individual can reproduce, mutate or die. The waiting times for the next evolution event are exponentially distributed with the following parameters:

- $b(x)$ the *reproduction rate* of an individual of trait x
 - with probability $1 - p(x)$ the reproduction event is a clonal reproduction and another individual of trait x appears
 - with probability $p(x)$ the reproduction event is a mutation and the mutant is of (random) trait y distributed according to a probability kernel $m(x, dy)$ on \mathcal{X}
- $d(x) + \sum_{i=1}^{N_t} c(x, x_i(t))$ is the *total death rate* for an individual of trait x , where $d(x)$ denotes the *natural death rate* and $\sum_{i=1}^{N_t} c(x, x_i(t))$ *death rate due to competition* of an individual of trait x caused by the presence of the N_t other individuals

Note that no a priori fitness is given. The selection process and the proper definition of fitness emerges from the interaction between individuals and competition for limited resources.

The models discussed above involve three natural *scaling parameters* that are biologically reasonable:

1. large population size, K . This is achieved by reducing competition by replacing $c(x, y)$ by $c(x, y)/K$. To obtain asymptotic results in the limit when $K \rightarrow \infty$, this requires to also replace the measures ν by their rescaled version $\nu^K \equiv \nu/K$.
2. small mutation probability, μ . This is achieved by replacing $p(x)$ by $\mu p(x)$.
3. small mutation steps, σ . The mutant is of trait $y = x + \sigma h$ where h is chosen according to a probability kernel on \mathcal{X} . For birth and death rates that vary smoothly on \mathcal{X} , this ensures a vanishing evolutionary advantage (if any) of mutants, when $\sigma \rightarrow 0$.

Let us briefly summarize the the main results that were obtained for these models.

- In the limit of large populations ($K \rightarrow \infty$ and μ, σ fixed) Fournier and Méléard [18] proved a law of large numbers: the process converges to a system of deterministic integro-differential equations. In the case $\mu \equiv 0$ the process converges to the solution of a system of coupled logistic equations (of Lotka-Volterra type) without mutations.

- The limit of large populations ($K \rightarrow \infty$) followed by the limit of rare mutations ($\mu \rightarrow 0$ with σ fixed) but on the timescale $t \sim \log(1/\mu)$ was studied by Bovier and Wang [6] and a deterministic jump process is obtained as limiting behavior.
- The simultaneous limit of large populations and rare mutations, where $(K, \mu) \rightarrow (\infty, 0)$ at a rate such that $1/(K\mu) \gg \log K$ and a timescale $t \sim 1/(K\mu)$ was studied by Champagnat and Méléard [8, 12]. At this scale the system has time to equilibrate between two successive mutations. In this situation, the long-term behaviour of the population can be described, on an appropriate time scale, as a Markov jump process along a sequence of equilibria of, in general, polymorphic populations. This process is called the *Polymorphic Evolution Sequence* (PES). An important (and in some sense generic) special case occurs when the mutant population fixates while resident population dies out in each step. The corresponding jump process is called the *Trait Substitution Sequence* (TSS) in adaptive dynamics. Champagnat [8] derived criteria in the context of individual-based models under which convergence to the TSS can be proven. Note that the description of the general PES is partly implicit, as it involves the identification of attractive fixed points in a sequence of Lotka-Volterra equations that are in general not tractable analytically.
- In situations when the population converges to a TSS, one may take a further limit of small mutation steps ($\sigma \rightarrow 0$) to derive the so-called *Canonical Equation of Adaptive Dynamics* (CEAD), see e. g. Champagnat [9], which describe the continuous evolution of a monomorphic population in a fitness landscape.
- The convergence to the CEAD has recently also been shown by Baar et al. [3] in the simultaneous limit of large populations, rare mutation and small mutation steps, where $(K, \mu, \sigma) \rightarrow (\infty, 0, 0)$, provided $1/(K\mu) \gg \log(K)/\sigma$ and $1/\sqrt{K} \ll \sigma \ll 1$. The time-scale on which this convergence takes place is $t \sim 1/(K\mu\sigma^2)$.
- Costa et al. [14] study the impact of natural selection on the coevolution of a prey-predator community (of d different traits of prey and m different traits of predators at each time). In addition to the usual birth, death and competition parameters, the predator-prey relation is modelled by a kernel acting as a death rate for preys, but as a birth rate for predators. This kernel is an explicit function of parameters describing for each trait of prey defence strategies, and for each trait of predator the ability of predators to circumvent the defence mechanism. Three different limit behaviours are considered: first, for $\mu = 0$ and $K \rightarrow \infty$, convergence in law to a system of differential equations holds; second, as $(K, \mu) \rightarrow (\infty, 0)$ at a rate such that $1/(K\mu) \gg \log K$, convergence in finite dimensional distribution to a Markov jump process generalizing the *Polymorphic Evolution Sequence* holds, and third, in the subsequent limit $\sigma \rightarrow 0$, at a timescale divided by σ^2 and in the case of a monomorphic prey and monomorphic predator population, convergence to an extended version of the CEAD is obtained.

1.3 Outline of the objective of the model

In the model we present in the next chapter, four main differences to the models explained above are included:

- Two types of transitions are allowed: genotypic mutations and phenotypic switches. The characteristic timescale for a mutation to occur can be significantly longer than a timescale for epigenetic transitions.
- Phenotypic changes may be affected by the environment which is not modelled deterministically as in [11] but as particles undergoing the random dynamics as well.
- A predator-prey mechanism is included (modelling the interaction of cancer cells and immune cells). The defence strategies of the prey are not modelled by different interaction rates as in [14] but by actually modelling the escape strategy, namely switching.
- A birth-reducing competition term is included which takes account of the fact that competition between individuals may also affect their reproduction behavior.

The inclusion of different kinds of transitions (switch and mutations) allows to extract an effective Markov chain on the space of genotypes, whose transition rates are given by the asymptotic

behavior of a faster Markov process on the space of phenotypes. The switch also has a strong influence on the behaviour of the corresponding deterministic system which is quite hard to analyse in general. In Section 4, we illustrate the effect of the above mentioned points through several examples.

A first example is the actual therapy carried out in [30]. We observe here a metastability phenomenon: in a phase of small predator and prey populations the predators can die out, allowing for a growth of the prey community. For the T-cell therapy we observe relapses consisting of different ratios of differentiated and dedifferentiated melanoma cells and appearing at random times. As a second example we study the T-cell therapy with 2 types of T-cells. In this case an ever richer class of possible behaviour occurs: either the tumor dies out, or one kind of T-cells dies out, or both kinds of T-cells die out or all populations survive for a given time. The next examples are devoted to the interplay of switch and mutation, that is one step of the effective Markov chain in the genotypic space mentioned above, and suggest a definition of fitness in this setting. In particular, we show that the usually used invasion fitness leads to wrong predictions on which mutants can survive. Some counterintuitive scenarios are illustrated. Last but not least we study the influence of the birth-reducing-competition on the mutation timescale. There are parameter regimes where mutations are not most likely to happen in the biggest populations. Combined with tumor therapy this yields an example where therapy-induced remission of a tumor can lead to a mutated more aggressive type of cancer cells.

2 The model

We introduce a general model, which contains three types of actors:

- *Cancer cells (melanoma)*: each cell is characterized by a genotype and a phenotype. These cells can reproduce, die, mutate (change genotype) or switch (change phenotype) at prescribed rates.
- *T-cells*: these cells can reproduce, die, kill a cancer cell of a prescribed type or produce a chemical messenger, at prescribed rates.
- *Chemical messenger TNF- α* : this messenger can die at a prescribed rate. Its presence influences the ability of a prescribed type of cancer cell to switch.

The trait space is a finite set of the form:

$$\mathcal{X} = \mathcal{G} \times \mathcal{P} \cup \mathcal{Z} \cup \mathcal{W} = \{g_1, \dots, g_{|\mathcal{G}|}\} \times \{p_1, \dots, p_{|\mathcal{P}|}\} \cup \{z_1, \dots, z_{|\mathcal{Z}|}\} \cup w \quad (2.1)$$

where $(g, p) \in \mathcal{G} \times \mathcal{P}$ stands for a melanoma with genotype g and phenotype p , $z \in \mathcal{Z}$ stands for a T-cell of type z and w stands for the TNF- α . We write $|\cdot|$ for the number of elements of a set and \cup for disjoint unions of sets. Interactions take place between $\mathcal{G} \times \mathcal{P}$, \mathcal{Z} and \mathcal{W} but there are no transitions allowed between these different “blocks”. Note that \mathcal{X} is a finite set and thus the power set can be used as a σ -algebra for the corresponding probability space. With this trait space we are able to treat the cases that different genotypes can have the same phenotype and vice versa.

2.1 General notations

A *population* at time $t \in \mathbb{R}_+$ is described by the measure

$$\nu_t = \sum_{x \in \mathcal{X}} \nu_t(x) \delta_x, \quad (2.2)$$

where $\nu_t(x)$ is the number of individuals of type x at time t . ν_t belongs to the space \mathcal{M} of integer valued measures on \mathcal{X} .

We assume that the birth rates, death rates and competition kernels depend only on phenotypes. We therefore introduce a short notation for the total number of melanoma cells with a given phenotype:

$$\nu_t(p) := \sum_{g \in \mathcal{G}} \nu_t(g, p), \quad (2.3)$$

where we write $\nu_t(g, p) := \nu_t((g, p))$. Therapy and production kernels of T-cells depend also only on phenotypes, as they biologically depend on the presence of specific markers on the surface of melanoma cells. The mutation and switch kernels are indexed by both, genotypes and phenotypes. More precisely,

1. Each type of cancer cell (g, p) is characterised by
 - $b(p) \in \mathbb{R}^+$ birth rate of a melanoma of type (g, p) ,
 - $d(p) \in \mathbb{R}^+$ death rate of a melanoma of type (g, p) ,
 - $c(p, \tilde{p}) \in \mathbb{R}^+$ competition kernel which causes an additional death rate of a melanoma cell of phenotype p in presence of a melanoma cell of phenotype \tilde{p} ,
 - $c_b(p, \tilde{p}) \in \mathbb{R}^+$ birth-reducing competition, i.e. competition kernel which lowers the birth rate of a melanoma cell of phenotype p in presence of a melanoma cell of phenotype \tilde{p} . If the total birth rate is already at a level 0, then this competition kernel is an additional death rate,
 - $t(z, p) \in \mathbb{R}^+$ therapy kernel which causes an additional death rate of a melanoma cell of phenotype p due to the presence of a T-cell of type z ,
 - $s^g(p, \tilde{p}) \in \mathbb{R}^+$ natural phenotypic switch kernel of a melanoma cell of type (g, p) to a melanoma cell of type (g, \tilde{p}) ,
 - $s_w^g(p, \tilde{p}) \in \mathbb{R}^+$ phenotypic switch kernel due to the presence of TNF- α of a melanoma cell of type (g, p) to a melanoma cell of type (g, \tilde{p}) ,
 - $\mu_g \in [0, 1]$ mutation probability of melanoma cells of genotype g ,
 - $m((g, p), (\tilde{g}, \tilde{p})) \in [0, 1]$ mutation kernel which encodes the probability that, whenever a mutation event occurs, a melanoma cell of type (g, p) gives birth to a melanoma cell of type (\tilde{g}, \tilde{p}) . $\sum_{\tilde{g}, \tilde{p}} m((g, p), (\tilde{g}, \tilde{p})) = 1$. By definition $m((g, p), (g, p)) = 0$
2. Each type of T-cell z is characterised by
 - $b(z) \in \mathbb{R}^+$ natural birth rate of a T-cell of type z ,
 - $b(z, p) \in \mathbb{R}^+$ the reproduction kernel of a T-cell with trait z in presence of a melanoma cell of phenotype p ,
 - $d(z) \in \mathbb{R}^+$ death rate of a T-cell of type z .
3. TNF- α proteins are characterised by
 - $\ell_w(z) \in \mathbb{N}$ number of TNF- α produced when a T-cell of type z is produced (not at “natural” birth events),
 - $\ell_w(z, p) \in \mathbb{N}$ number of TNF- α produced when a T-cell with trait z kills a melanoma cell of phenotype p ,
 - $d(w) \in \mathbb{R}^+$ natural death rate of TNF- α .

Remark 2 Note that $\mathcal{G} \times \mathcal{P}$ allows for any combination of genotype and phenotype and no a priori translation from \mathcal{G} to \mathcal{P} or vice versa is assumed. The relation of \mathcal{G} and \mathcal{P} is encoded in the switch kernels which specify which phenotypes are expressed by a given genotype in a (dynamic) environment.

2.2 The dynamics

We are interested in the evolution of the random point measure ν_t , describing the evolution of the population at each time t . Let $[\cdot]_+$ and $[\cdot]_-$ denote the positive or negative part of the argument, respectively. The dynamics of the population can be summarized as follows. The initial population

is characterized by a measure ν_0 at time $t = 0$, and each individual with trait $x \in \mathcal{X}$ at time t has several exponential clocks with intensities depending on the current state of the system:

1. Each melanoma cell of trait $(g, p) \in \mathcal{G} \times \mathcal{P}$ has
 - a “clonal reproduction” clock with rate

$$(1 - \mu_g) \left[b(p) - \sum_{\tilde{p} \in \mathcal{P}} c_b(p, \tilde{p}) \nu_t(\tilde{p}) \right]_+, \quad (2.4)$$

- a “mutant reproduction” clock with rate

$$\mu_g \left[b(p) - \sum_{\tilde{p} \in \mathcal{P}} c_b(p, \tilde{p}) \nu_t(\tilde{p}) \right]_+, \quad (2.5)$$

- a “natural mortality” clock with rate

$$d(p) + \sum_{\tilde{p} \in \mathcal{P}} c(\tilde{p}, p) \nu_t(\tilde{p}) + \left[b(p) - \sum_{\tilde{p} \in \mathcal{P}} c_b(p, \tilde{p}) \nu_t(\tilde{p}) \right]_-, \quad (2.6)$$

- a “therapy mortality” clock of rate

$$\sum_{z \in \mathcal{Z}} t(z, p) \nu_t(z), \quad (2.7)$$

- a “TNF- α induced switch” clock of rate

$$\sum_{\tilde{p} \in \mathcal{P}} s_w^g(p, \tilde{p}) \nu_t(w), \quad (2.8)$$

- and a “natural switch” clock of rate

$$\sum_{\tilde{p} \in \mathcal{P}} s^g(p, \tilde{p}). \quad (2.9)$$

If the “clonal reproduction” clock rings, then it produces an individual with the same trait (g, p) ; if the “mutant reproduction” clock of a (g, p) individual rings, then it produces an individual with characteristics (\tilde{g}, \tilde{p}) according to the kernel $m((g, p), (\tilde{g}, \tilde{p}))$. If one of the “mortality” clocks of a (g, p) individual rings, then this individual disappears. If the mortality which rings is a “therapy mortality” clock, then an addition $\ell_w(g, p)$ TNF- α appear. If the “natural switch” clock or the “TNF- α induced switch” clock of a (g, p) individual rings, then this individual disappears and a new individual of trait (g, \tilde{p}) appears where \tilde{p} is distributed according to the corresponding kernel $s^g(p, \tilde{p})$ or $s_w^g(p, \tilde{p})$.

2. Each T-cell of trait $z \in \mathcal{Z}$ has

- a “natural birth” clock and a natural “mortality” clock with rates

$$b(z) \quad \text{and} \quad d(z) \quad (2.10)$$

- and a “reproduction” clock with rate

$$\sum_{p \in \mathcal{P}} b(z, p) \nu_t(p). \quad (2.11)$$

If the “reproduction” clock of a T-cell rings, then it produces a T-cell with the same trait z and $\ell_w(z)$ TNF- α appear.

3. Each TNF- α has

- a “mortality” clock with rate $d(w)$

- Moreover, an amount of $\ell_w(z, p)$ particles (of trait w) are produced every time a T-cell of trait z kills a melanoma cell of trait (g, p) , and a number of $\ell_w(z)$ particles are produced every time a T-cell of trait z is produced.

We introduce a parameter K in order to scale the population size. This parameter, in the case of competition for resources, is called carrying capacity of the environment, and can be interpreted as scaling the amount of available resources, so that an increase of K implies a decrease of the strength of competition for resources between two individuals.

We thus introduce the following scaling of the parameters. For each $K \in \mathbb{N}$, we keep all parameters unchanged, except those in front of quadratic terms (that is $c_b(\cdot, \cdot)$, $c(\cdot, \cdot)$, $t(\cdot, \cdot)$, $s_w^g(\cdot, \cdot)$ and $b(\cdot, \cdot)$) which we rescale by a factor $1/K$. We are interested in the rescaled measure

$$\nu_t^K = \frac{1}{K} \sum_{i=1}^{N_t} \delta_{x_i(t)}. \quad (2.12)$$

which belongs to the space of measures $\mathcal{M}^K(\mathcal{X}) = \{\frac{1}{K} \sum_{i=1}^n \delta_{x_i} : n \in \mathbb{N}, x_1, \dots, x_n \in \mathcal{X}\}$. The measure-valued process $(\nu_t^K)_{t \geq 0}$ is a Markov process whose law is characterized by its infinitesimal generator L^K which captures the dynamics described above (cf. [17] and [18]). The generator of the rescaled process acts on functions ϕ from \mathcal{M}^K into \mathbb{R} , for all $\nu \in \mathcal{M}^K$ by

$$\begin{aligned} (L^K \phi)(\nu) &= \sum_{(g,p) \in \mathcal{G} \times \mathcal{P}} \left(\phi \left(\nu + \frac{\delta_{(g,p)}}{K} \right) - \phi(\nu) \right) (1 - \mu_g) \left[b(p) - \sum_{\tilde{p} \in \mathcal{P}} c_b(p, \tilde{p}) \nu(\tilde{p}) \right]_+ K \nu(g, p) \\ &+ \sum_{(g,p) \in \mathcal{G} \times \mathcal{P}} \left(\phi \left(\nu - \frac{\delta_{(g,p)}}{K} \right) - \phi(\nu) \right) \left(d(p) + \sum_{\tilde{p} \in \mathcal{P}} c(p, \tilde{p}) \nu(\tilde{p}) \right. \\ &\quad \left. + \left[b(p) - \sum_{\tilde{p} \in \mathcal{P}} c_b(p, \tilde{p}) \nu(\tilde{p}) \right]_- \right) K \nu(g, p) \\ &+ \sum_{(g,p) \in \mathcal{G} \times \mathcal{P}} \left(\phi \left(\left(\nu - \frac{\delta_{(g,p)}}{K} + \ell_w(z, p) \frac{\delta_w}{K} \right) - \phi(\nu) \right) \left(\sum_{z \in \mathcal{Z}} t(z, p) \nu(z) \right) K \nu(g, p) \right. \\ &+ \sum_{(g,p) \in \mathcal{G} \times \mathcal{P}} \sum_{\tilde{p} \in \mathcal{P}} \left(\phi \left(\nu + \frac{\delta_{(g,\tilde{p})}}{K} - \frac{\delta_{(g,p)}}{K} \right) - \phi(\nu) \right) \left(s^g(p, \tilde{p}) + s_w^g(p, \tilde{p}) \nu(w) \right) K \nu(g, p) \\ &+ \sum_{z \in \mathcal{Z}} \left(\phi \left(\nu + \frac{\delta_z}{K} + \ell_w(z) \frac{\delta_w}{K} \right) - \phi(\nu) \right) \left(\sum_{p \in \mathcal{P}} b(z, p) \nu(p) \right) K \nu(z) \\ &+ \sum_{z \in \mathcal{Z}} \left(\phi \left(\nu + \frac{\delta_z}{K} \right) - \phi(\nu) \right) b(z) K \nu(z) \\ &+ \sum_{z \in \mathcal{Z}} \left(\phi \left(\nu - \frac{\delta_z}{K} \right) - \phi(\nu) \right) d(z) K \nu(z) \\ &+ \left(\phi \left(\nu - \frac{\delta_w}{K} \right) - \phi(\nu) \right) d(w) K \nu(w) \\ &+ \sum_{(\tilde{g}, \tilde{p}) \in \mathcal{G} \times \mathcal{P}} \sum_{(g,p) \in \mathcal{G} \times \mathcal{P}} \left(\phi \left(\nu + \frac{\delta_{(\tilde{g}, \tilde{p})}}{K} \right) - \phi(\nu) \right) \\ &\quad \times \mu_g m((g, p), (\tilde{g}, \tilde{p})) \left[b(p) - \sum_{p' \in \mathcal{P}} c_b(p, p') \nu(p') \right]_+ K \nu(g, p) \end{aligned} \quad (2.13)$$

2.3 Simulation

All the figures of this article containing simulations of the above model were generated by a computer program written by Boris Prochnau.

3 Convergence result

Let us now consider the above mentioned rescaled process in which the number of particles increases with K , and the parameters in front of linear terms stay unchanged, whereas the parameters in front of quadratic terms tends to zero as $1/K$. We show that the process ν_t^K can be approximated by a deterministic function, moreover by the solution of a quadratic system of ODE.

We see \mathcal{M}^K as a subset of the set $\mathcal{M}_F(\mathcal{X})$ of finite non-negative measures on \mathcal{X} , endowed with the weak topology. The population can be represented as a vector $V_K(t) := (\nu_t^K(x))_{x \in \mathcal{X}}$ of dimension $d = |\mathcal{G}| \cdot |\mathcal{P}| + |\mathcal{Z}| + 1$. Moreover, there is a natural way to jointly construct the processes for different values of K , see [17]. For this coupling, we have the following result.

Theorem 1 *Suppose that the initial conditions converge almost surely to a deterministic limit, i.e. $\lim_{K \rightarrow \infty} V_K(0) = v(0)$. Then, for each $T \in \mathbb{R}_+$ the rescaled process $(V_K(t))_{0 \leq t \leq T}$ converges almost surely as $K \rightarrow \infty$ to the d -dimensional deterministic process which is the unique solution to the following quadratic dynamical system:*

$$\begin{aligned}
\frac{d\mathbf{n}_{(g,p)}}{dt} &= \left((1 - \mu_g) \left[b(p) - \sum_{(\tilde{g}, \tilde{p}) \in \mathcal{G} \times \mathcal{P}} c_b(p, \tilde{p}) \mathbf{n}_{(\tilde{g}, \tilde{p})} \right]_+ - \left[b(p) - \sum_{(\tilde{g}, \tilde{p}) \in \mathcal{G} \times \mathcal{P}} c_b(p, \tilde{p}) \mathbf{n}_{(\tilde{g}, \tilde{p})} \right]_- \right. \\
&\quad \left. - d(p) - \sum_{(\tilde{g}, \tilde{p}) \in \mathcal{G} \times \mathcal{P}} c(p, \tilde{p}) \mathbf{n}_{(\tilde{g}, \tilde{p})} - \sum_{z \in \mathcal{Z}} t(z, p) \mathbf{n}_z - \sum_{\tilde{p} \in \mathcal{P}} (s^g(p, \tilde{p}) + s_w^g(p, \tilde{p}) \mathbf{n}_w) \right) \mathbf{n}_{(g,p)} \\
&\quad + \sum_{\tilde{p} \in \mathcal{P}} (s^g(\tilde{p}, p) + s_w^g(\tilde{p}, p) \mathbf{n}_w) \mathbf{n}_{(g, \tilde{p})} \\
&\quad + \sum_{(\tilde{g}, \tilde{p}) \in \mathcal{G} \times \mathcal{P}} \left(\mu_{\tilde{g}} m((\tilde{g}, \tilde{p}), (g, p)) \left[b(\tilde{p}) - \sum_{(g', p') \in \mathcal{G} \times \mathcal{P}} c_b(\tilde{p}, p') \mathbf{n}_{(g', p')} \right]_+ \right) \mathbf{n}_{(\tilde{g}, \tilde{p})} \\
\frac{d\mathbf{n}_z}{dt} &= \left(b(z) - d(z) + \sum_{(g,p) \in \mathcal{G} \times \mathcal{P}} b(z, p) \mathbf{n}_{(g,p)} \right) \mathbf{n}_z \\
\frac{d\mathbf{n}_w}{dt} &= -d(w) \mathbf{n}_w + \sum_{(g,p) \in \mathcal{G} \times \mathcal{P}} \left(\sum_{z \in \mathcal{Z}} (\ell_w(z, p) t(z, p) + \ell_w(z) b(z, p)) \mathbf{n}_z \mathbf{n}_{(g,p)} \right). \tag{3.1}
\end{aligned}$$

More precisely, $\mathbb{P}(\lim_{K \rightarrow \infty} \sup_{0 \leq t \leq T} |V_K(t) - \mathbf{n}(t)| = 0) = 1$, where $\mathbf{n}(t)$ denotes the solution to Equations (3.1) with initial condition $v(0)$.

Proof The process $V_K(t)$ can be constructed explicitly from a finite collection of Poisson processes, where to each possible event corresponds a Poisson Process Y_l . The index $l \in \mathbb{Z}^d$ encodes the possible transitions between (non-rescaled) population states and $\beta_l : \mathbb{R}^d \rightarrow \mathbb{R}$ is a function yielding the corresponding transition rates. Let us denote by e_i the i -th unit vector and by v_i denotes the i -th entry of the vector $v \in \mathbb{R}^d$. With a slight abuse of notation, the different possible events, their corresponding l and β_l for a population in state $v \in \mathbb{R}^d$ are

1. Type i birth (clonal or mutational): $l = e_i$, with

$$\beta_l(v) = (1 - \mu_i) \left[b(i) - \sum_{k=1}^{|\mathcal{G}| |\mathcal{P}|} c_b(i, k) v_k \right]_+ v_i$$

$$+ \sum_{k=1}^{|\mathcal{G}||\mathcal{P}|} \left(\mu_k m(k, i) \left[b(k) - \sum_{m=1}^{|\mathcal{G}||\mathcal{P}|} c_b(k, m) v_m \right]_+ \right) v_k, \quad (3.2)$$

and $\beta_l(v) = b(i)$ if i refers to a T-cell population

2. Type i T-cell production combined with TNF- α production: $l = e_i + \ell_w(z)e_d$, with $\beta_l(v) = \left(\sum_{k=1}^{|\mathcal{G}||\mathcal{P}|} b(i, k) v_k \right) v_i$
3. Type i death (natural or due to competition): $l_i = -e_i$ with $\beta_l(v) = \left(d(i) + \sum_{k=1}^{|\mathcal{G}||\mathcal{P}|} c(i, k) v_k + \left[b(i) - \sum_{k=1}^{|\mathcal{G}||\mathcal{P}|} c_b(i, k) v_k \right]_- \right) v_i$
4. Type i Melanoma killing event combined with TNF- α production: $l_i = -e_i + \ell_w(z)e_d$, with $\beta_l(v) = \sum_{z=1}^{|\mathcal{Z}|} t(z, i) v_z v_i$
5. Type i to type j switching event, $l = -e_i + e_j$ with $\beta_l(v) = (s(i, j) + s_w(i, j) v_d) v_i$

For transitions not mentioned above $\beta_l(v) = 0$. Furthermore, $V_K(t)$ satisfies

$$V_K(t) = V_K(0) + \sum_l l K^{-1} \tilde{Y}_l(K\beta_l(V_K(s)) ds) + \int_0^t F(V_K(s)) ds, \quad (3.3)$$

where $\tilde{Y}_l(u) = Y_l(u) - u$ is the Poisson process centered at its expectation and $F(v) \equiv \sum_l l\beta_l(v)$ for $v \in \mathbb{R}^d$. Since we have only finitely many possible transitions and all event rates are finite,

$$\sum_l |l| \sup_{v \in \mathbb{R}^d} \beta_l(v) < \infty. \quad (3.4)$$

Moreover, $F(v)$ is Lipschitz continuous on compact subsets of \mathbb{R}_+^d and $\mathbf{n}(t)$ satisfies for every $t \geq 0$

$$\mathbf{n}(t) = v(0) + \int_0^t F(\mathbf{n}(s)) ds. \quad (3.5)$$

Thus, the claimed result follows directly from Theorem 2.1 in Chapter 11 of [17]. \square

4 Key examples

4.1 Different relapse behaviour due to random fluctuations

4.1.1 Therapy with T-cells with one specificity

This example aims at qualitatively explaining the behaviour of the model for the scenario of melanoma escaping treatment with adoptive cell transfer by switching their phenotype in the presence of TNF- α . Biologically reasonable parameters are found in Section 5. In this experiment, only one type of T-cells was used: the ones that can only kill differentiated cancer cells. To keep the picture clear and since this was not investigated in the experiments, we do not consider mutations here.

Let us denote by $x := (g, p)$ the differentiated cancer cells, $y := (g, p')$ the dedifferentiated cancer cells, z the T-cells, and w the TNF- α proteins. The dynamics of the model can be explained more easily in the corresponding deterministic system obtained in the limit of large populations ($K \rightarrow \infty$) and given by Theorem 1:

$$\begin{cases} \dot{\mathbf{n}}_x = \mathbf{n}_x (b(x) - d(x) - c(x, x)\mathbf{n}_x - c(x, y)\mathbf{n}_y - s(x, y) - s_w(x, y)\mathbf{n}_w - t(z, x)\mathbf{n}_z) + s(y, x)\mathbf{n}_y \\ \dot{\mathbf{n}}_y = \mathbf{n}_y (b(y) - d(y) - c(y, y)\mathbf{n}_y - c(y, x)\mathbf{n}_x - s(y, x)) + s(x, y)\mathbf{n}_x + s_w(x, y)\mathbf{n}_w\mathbf{n}_x \\ \dot{\mathbf{n}}_z = (b(z, x)\mathbf{n}_x - d(z))\mathbf{n}_z \\ \dot{\mathbf{n}}_w = (\ell_w(z, x)t(z, x) + \ell_w(z)b(z, x))\mathbf{n}_x\mathbf{n}_z - d(w)\mathbf{n}_w \end{cases} \quad (4.1)$$

Depending on the choice of the parameters there can exist a stable fixed point where all subpopulations are present at a non-zero level. For example, for the following parameter choice the behaviour of the system is qualitatively shown in Figure 2:

$$\begin{aligned}
 b(x) &= 3 & b(y) &= 3 & b(z, x) &= 8 & \ell_w(z, x) &= 1 \\
 d(x) &= 1 & d(y) &= 1 & t(z, x) &= 28 & d(w) &= 15 \\
 c(x, x) &= 0.3 & c(y, x) &= 0 & d(z) &= 3 & s_w(x, y) &= 4 \\
 c(x, y) &= 0 & c(y, y) &= 0.3 & & & & \\
 s(x, y) &= 0 & s(y, x) &= 1 & & & & \\
 \mathbf{n}_x(0) &= 2 & \mathbf{n}_y(0) &= 0 & \mathbf{n}_z(0) &= 0.05 & K &= 200
 \end{aligned} \tag{4.2}$$

The initial conditions at the start of tumor therapy are usually a large number of tumor cells $\mathbf{n}_x(0)$ and a small number of injected T-cells $\mathbf{n}_z(0)$ while $\mathbf{n}_y(0)$ and $\mathbf{n}_w(0)$ are zero or very small. The solution of the dynamical system (4.1) with parameters (4.2) as shown in Figure 2 can be described as follows: the T-cell population z increases in presence of its target x , it causes the growth of the TNF- α population w , and the decay of the melanoma population of type x by killing these cells. The presence of w induces the switch from x to y and the melanoma population of type y is not affected by the T-cells z . The equilibrium of the whole system is a large value of y , a small value of x , and small positive values of z and w . Depending on the choice of parameters also other scenarios are possible, e.g. the ratio of x and y populations could be very different.

The system (4.1) with parameter (4.2) has 4 fixed points: The trivial fixed point $\mathbf{n}_1 = (0, 0, 0, 0)$, and $\mathbf{n}_2 = (\bar{\mathbf{n}}_x^2, 0, 0, 0)$, $\mathbf{n}_3 = (\bar{\mathbf{n}}_x^3, \bar{\mathbf{n}}_y^3, 0, 0)$ and $\mathbf{n}_4 = (\bar{\mathbf{n}}_x^4, \bar{\mathbf{n}}_y^4, \bar{\mathbf{n}}_z^4, \bar{\mathbf{n}}_w^4)$ with all entries positive. Note that the subspace $\{\mathbf{n}_z = 0\}$ is invariant under the dynamics.

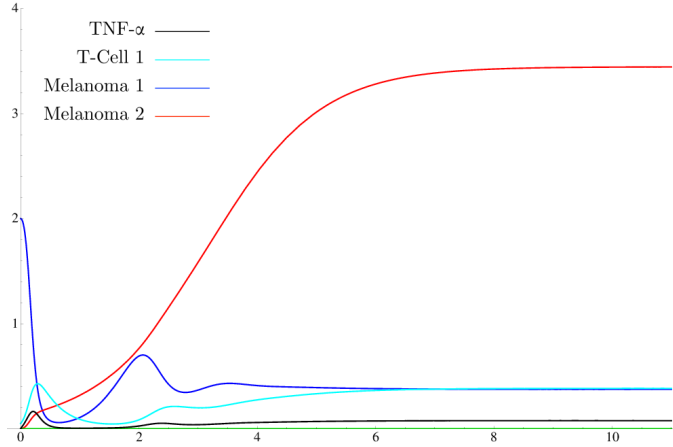


Fig. 2: The deterministic system.

One important difference between the deterministic system and the corresponding stochastic system is that populations that once appeared cannot die out in the deterministic but can die out in the stochastic system. Two reasons for the extinction of a population in the stochastic system are possible: first, the population size passes through a very low minimum of the deterministic system. Depending on the total population size K in the stochastic system the probability to die out can be high and only upwards fluctuations lead to survival of this population. Second, the equilibrium value for a population can be small but positive and downwards fluctuations lead to the extinction of a population. For the stochastic model (finite populations) and the parameters used above the population z fluctuates around its small minimum of the corresponding deterministic system. If the T-cell population, z , dies out (due to a downward fluctuation), the TNF- α population, w , dies shortly afterwards and the population of differentiated melanoma cells, x , grows again because these cells are no longer killed by the T-cells and TNF- α is not there any more to induce the switch from x to y . So, we observe a relapse which consists mainly of differentiated cells, where x

and y both stabilise at their equilibria. This behaviour is shown on the right hand side of Figure 3. Depending on the parameter choice, in particular the switching or cross-competition parameters, different behaviour is possible, e.g. the population of type y may die out.

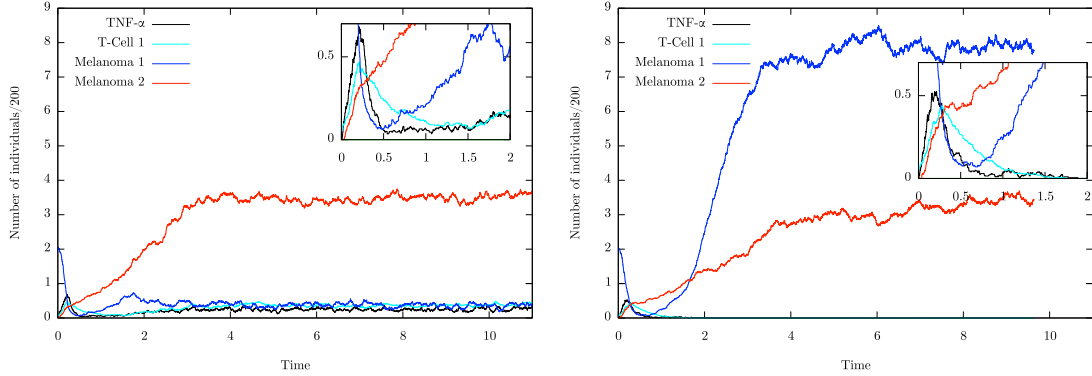


Fig. 3: Qualitative example of the stochastic choice between qualitatively different behaviors in the case of T-cell therapy with one specificity. (Left) T-cells do not die and the value of x stays small. (Right) T-cells die out and the relapse occurs.

The deterministic system predicts a unique behaviour of the tumor under therapy : the convergence to \mathbf{n}_4 , a relapse consisting mainly of melanoma cells of type y . For the stochastic system two scenarios are possible: either the convergence to \mathbf{n}_4 or, if the T-cells z die out (which happens with positive probability), the convergence to \mathbf{n}_3 .

Although we are studying a 4 dimensional system, it is interesting to observe the stochastic choice between qualitatively different behaviors on the vector field $(\dot{\mathbf{n}}_x, \dot{\mathbf{n}}_y, \dot{\mathbf{n}}_z, \dot{\mathbf{n}}_w)$ given by (4.1), by projecting it onto the first two coordinates (the two melanoma populations), as it is shown on Figure 4. The four fixed points of 4.1 for the given parameter choice are marked as blue dots. On the left of the figure, the vector field is drawn for $\mathbf{n}_w = \mathbf{n}_z = 0$ corresponding to fixed points \mathbf{n}_1 , \mathbf{n}_2 and \mathbf{n}_3 and on the right for $\mathbf{n}_w = \bar{\mathbf{n}}_w^4$ and $\mathbf{n}_z = \bar{\mathbf{n}}_z^4$. The picture shows that if the T-cells survive (right) the system is attracted to the fixed point where the number of x -melanoma cells is small, whereas if they die out (left) the system is attracted to the fixed point where the number of x -melanoma cells is large. These vector fields show already that \mathbf{n}_1 and \mathbf{n}_2 are unstable fixed points whereas the instability of \mathbf{n}_3 is hidden in the dimensions which are not shown in the pictures.

4.1.2 Therapy with T-cells with two different specificities

The dedifferentiated melanoma cells are also dangerous cancer cells and a therapy can only be called successful if the whole tumor is eradicated or kept small for a long time. Thus, Landsberg et al. [30] suggest to inject in future therapies two types of T-cells. By adapting the model for therapy with one type of T-cells to the setup of therapy with T-cells of two different specificities we can test this new therapy approach mathematically. The stochastic model for this situation undergoes a slightly more complicated stochastic choice between qualitatively different behaviors. We will denote in the following T-cells attacking the differentiated melanoma cells by z_x and T-cells

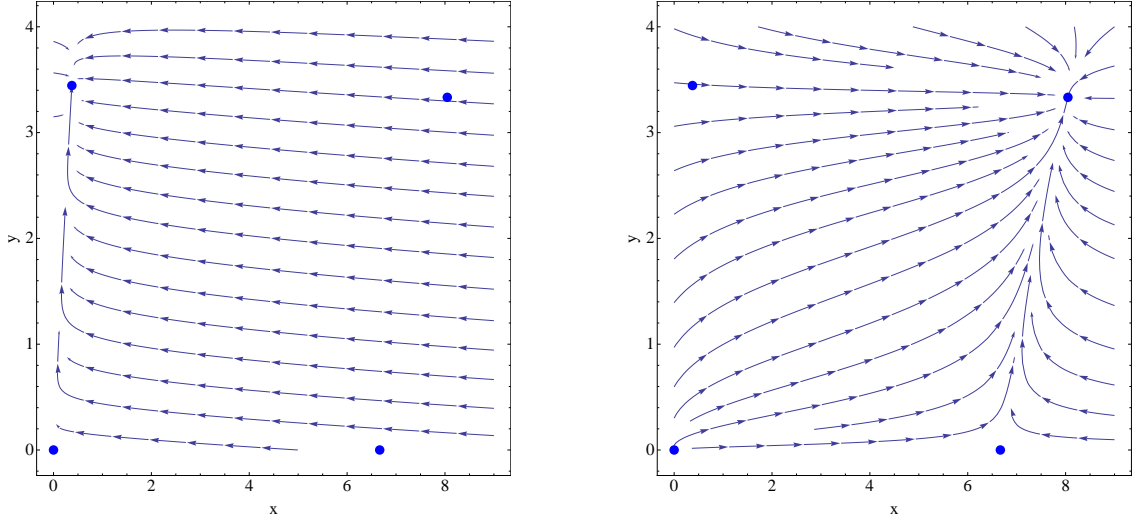


Fig. 4: Projection of the vector field $(\dot{\mathbf{n}}_x, \dot{\mathbf{n}}_y, \dot{\mathbf{n}}_z, \dot{\mathbf{n}}_w)$ given by (4.1) and parameters (4.2) onto the two first coordinates, (left) for $\mathbf{n}_z = \mathbf{n}_w = 0$, and (right) for $\mathbf{n}_z = \bar{\mathbf{n}}_z^4, \mathbf{n}_w = \bar{\mathbf{n}}_w^4$.

attacking the dedifferentiated melanoma cells by z_y . The deterministic system is described by the following equations:

$$\begin{cases} \dot{\mathbf{n}}_x = \mathbf{n}_x(b(x) - d(x) - c(x, x)\mathbf{n}_x - c(x, y)\mathbf{n}_y - s_w(x, y)\mathbf{n}_w - s(x, y) - t(z_x, x)\mathbf{n}_{z_x}) + s(y, x)\mathbf{n}_y \\ \dot{\mathbf{n}}_y = \mathbf{n}_y(b(y) - d(y) - c(y, y)\mathbf{n}_y - c(y, x)\mathbf{n}_x - s(y, x) - t(z_y, y)\mathbf{n}_{z_y}) + (s_w(x, y)\mathbf{n}_w + s(x, y))\mathbf{n}_x \\ \dot{\mathbf{n}}_{z_x} = \mathbf{n}_{z_x}(b(z_x, x)\mathbf{n}_x - d(z_x)) \\ \dot{\mathbf{n}}_{z_y} = \mathbf{n}_{z_y}(b(z_y, y)\mathbf{n}_y - d(z_y)) \\ \dot{\mathbf{n}}_w = (\ell_w(z_x, x)t(z_x, x) + \ell_w(z_x) b(z_x, x))\mathbf{n}_{z_x}\mathbf{n}_x \\ \quad + (\ell_w(z_y, y)t(z_y, y) + \ell_w(z_y) b(z_y, y))\mathbf{n}_{z_y}\mathbf{n}_y - d(w)\mathbf{n}_w \end{cases} \quad (4.3)$$

The solution of the dynamical system (4.3) is similar to the one explained in section 4.1.1, with the added effect of the second type of T-cells.

We can observe stochastic choice between six qualitatively different behaviors:

1. A cure, where all tumor and finally also all T-cells die out.
2. A relapse, where both T-cell populations die out and both melanoma populations survive.
3. A relapse, where the population of T-cells killing the differentiated cancer cells die out.
4. A relapse, where the population of T-cells killing the dedifferentiated cancer cells die out.
5. A relapse, where only the differentiated melanoma cells survive. (This is possible only when the natural switch term from x to y vanishes, i.e. $s(x, y) = 0$.)
6. A relapse, where all populations survive.

Depending on the choice of parameters these cases correspond to different behaviour: stable or unstable fixed points or cycles. Note that the subspaces $\{\mathbf{n}_{z_x} = 0\}$, $\{\mathbf{n}_{z_y} = 0\}$, and $\{\mathbf{n}_{z_x} = 0\} \cap \{\mathbf{n}_{z_y} = 0\}$ are invariant under the dynamics.

For the following parameter choice the equilibrium values of the two types of T-cells are low as shown in Figure 5, so they are both subject to fluctuations in the stochastic system.

$$\begin{array}{lllll}
 b(x) = 3 & b(y) = 3 & b(z_x, x) = 8 & b(z_y, y) = 14 & \ell_w(z_x, x) = 1 \\
 d(x) = 1 & d(y) = 1 & t(z_x, x) = 28 & t(z_y, y) = 28 & \ell_w(z_y, y) = 1 \\
 c(x, x) = 0.3 & c(y, x) = 0 & d(z_x) = 3 & d(z_y) = 3 & d(w) = 15 \\
 c(x, y) = 0 & c(y, y) = 0.3 & & & s_w(x, y) = 4 \\
 s(x, y) = 0 & s(y, x) = 1 & & & \\
 \mathbf{n}_x(0) = 2 & \mathbf{n}_y(0) = 0 & \mathbf{n}_{z_x}(0) = 0.05 & \mathbf{n}_{z_y}(0) = 2 & K = 200
 \end{array} \tag{4.4}$$

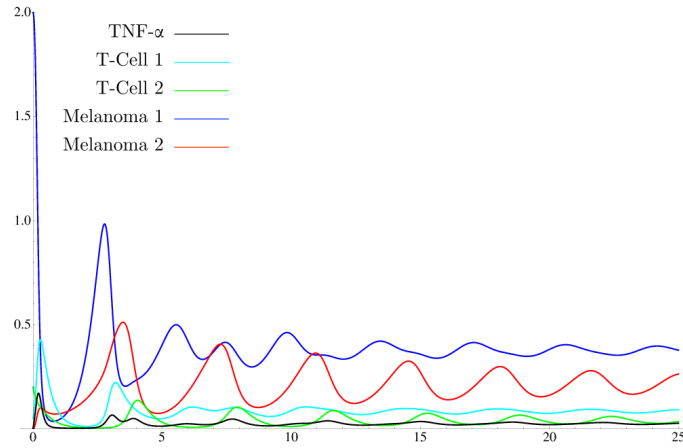


Fig. 5: The deterministic system

In Figure 6 the left-hand pictures shows the case where the simultaneous attack of the two different T-cell populations eradicates the tumor. Shortly after the extinction of the tumor also the T-cells and TNF- α die out since they are not produced any more in the absence of their target. On the right-hand side of this figure the tumor survives at a low level for some time. Note that the birth rate of the T-cells when the tumor is at a low level is very small, in particular smaller than their natural death rate ($b(z_x, x)\nu_t^K(x) < d(z_x)$ or $b(z_y, y)\nu_t^K(y) < d(z_y)$). All T-cells die out before the tumor grows again.

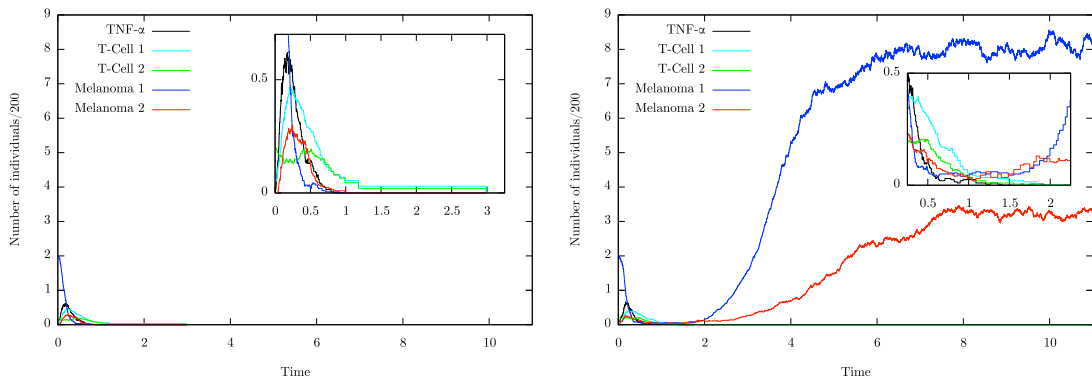


Fig. 6: Qualitative examples in the case of therapy with two T-cell types. (Left) Cure, all populations die out. (Right) Both types of T-cells die out.

In Figure 7 the cases where only one of the T-cell populations dies out are shown. In the case where the T-cells attacking the differentiated cells died out (on the left) the differentiated cells build the largest population although $\text{TNF-}\alpha$ is still produced by the other T-cell population and causing switching from differentiated cells to dedifferentiated cells. This “feeding” of this population decreases the probability that they will be extinct compared to a situation without switching. In the case when the T-cells attacking the dedifferentiated cells died out (on the right) the system tends to an equilibrium with a high proportion of dedifferentiated melanoma cells.

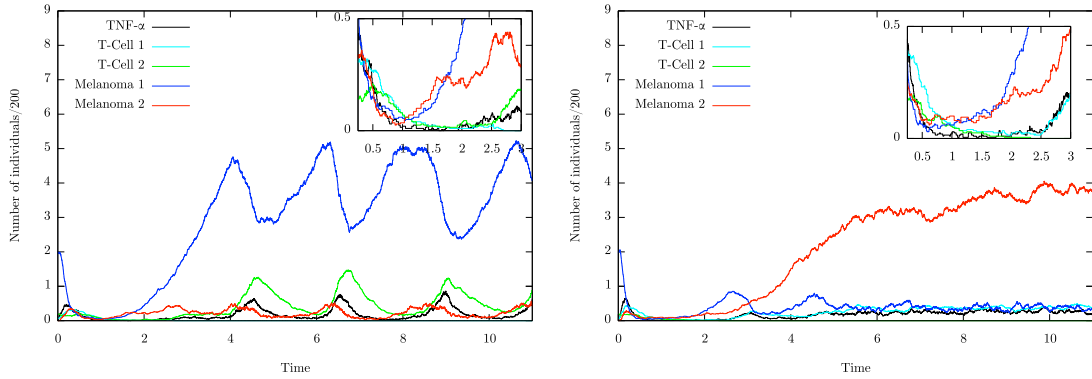


Fig. 7: Qualitative examples in the case of therapy with two T-cell types. (Left) T-cells attacking the differentiated melanoma cells die out. (Right) T-cells attacking the dedifferentiated melanoma cells die out.

It can happen that a cure is almost reached but very few differentiated cancer cells survive whereas the dedifferentiated cancer cells died out (on the left of Figure 8). Since for our parameter choice there is no natural switch from differentiated to dedifferentiated cells and no $\text{TNF-}\alpha$ is present any more the population of dedifferentiated cells cannot reappear. On the right of Figure 8 it is shown that it is possible that all populations survive for some time fluctuating around their joint equilibrium. Of course, it is always possible that some populations die out due to fluctuations which would bring the system to one of the other cases presented.

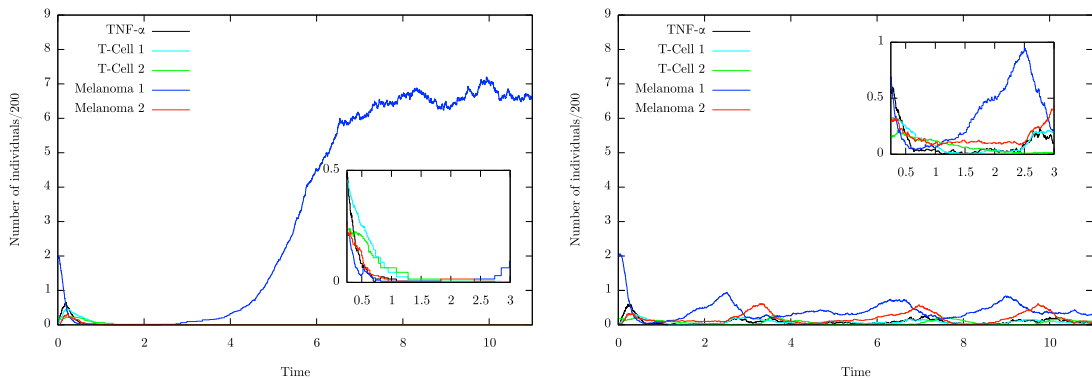


Fig. 8: Qualitative examples in the case of therapy with two T-cell types. (Left) All populations but the differentiated melanoma cells die out. (Right) All populations survive.

Two new fixed points appear in the system (4.3) with parameters (4.4) compared to the situation where only one T-cell type is considered. They are marked as red dots in Figure 9. Calculating the eigenvalues of the corresponding Jacobian matrix yields that only the fixed point where all populations survive is stable, all the other ones are unstable. This is partly visible in the corresponding vector fields in Figures 4 and 9 but the instability can also be “hidden” in a direction that is not shown for the plot of the vector field, e.g. for the red fixed point which seems to be stable on the left of Figure 9.

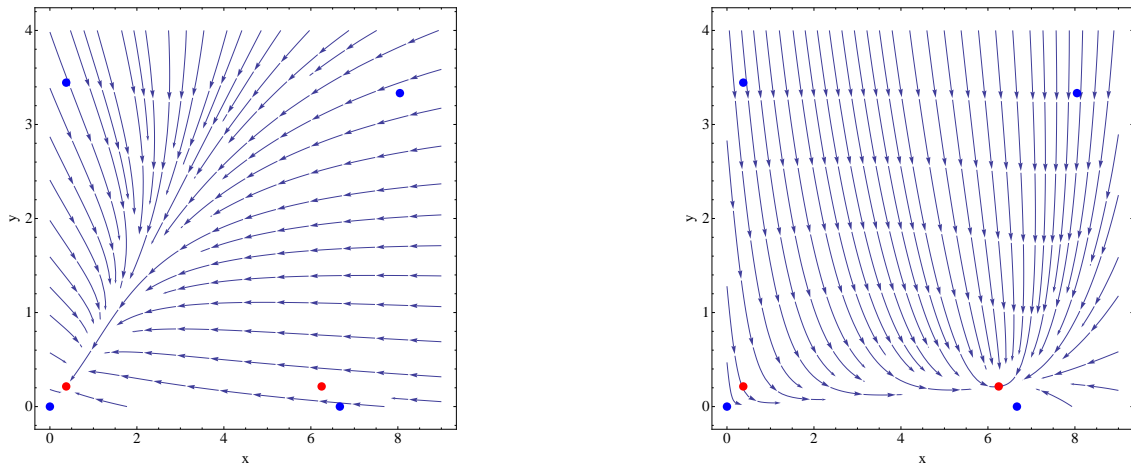


Fig. 9: Projection of the vector field $(\dot{n}_x, \dot{n}_y, \dot{n}_{z_x}, \dot{n}_{z_y}, \dot{n}_w)$ given by (4.3) and parameters (4.4) onto the two first coordinates, (left) for $n_{z_x} = n_{z_y} = n_w = 0$, and (right) for $n_{z_x} = \bar{n}_{z_x}, n_{z_y} = \bar{n}_{z_y}, n_w = \bar{n}_w$.

4.2 Arrival of a mutant.

A natural question to ask in the context of our models is what analogues of the PES and TSS processes that describe the long-term behaviour of the standard models for adaptive dynamics are. There are clearly a number of new difficulties that at the moment are only partly understood.

Invasion fitness. A fundamental concept used in the analysis of the stochastic population models described in Section 1.2 is that of *invasion fitness*: given a mono- or polymorphic population in equilibrium that populates a certain set of traits, say $M \subset \mathcal{X}$, the invasion fitness $f(x, M)$ is the growth rate of a population consisting of a single individual with trait $x \notin M$ in the presence of the equilibrium population \bar{n} on M . In the classical case it is simply given by

$$f(x, M) = b(x) - d(x) - \sum_{y \in M} c(x, y) \bar{n}_y. \quad (4.5)$$

Positive $f(x, M)$ implies that a mutant appearing with phenotype x from the equilibrium population on M has a positive probability (uniformly in K) to grow to a population of size of order K ; negative invasion fitness implies that such a mutant population will die out with probability tending to one (as $K \rightarrow \infty$) before this happens. We need to generalize this notion to the case when fast phenotypic switches are present. We show how this can be done in the case of pure tumor evolutions, i.e. we ignore the T-cells and the TNF- α . We consider an initial population of genotype g (associated with ℓ different phenotypes p_1, \dots, p_ℓ) which is able to mutate at rate μ to another genotype g' , associated with k different phenotypes p'_1, \dots, p'_k . The standard assumption (see e.g. Champagnat [8])

$$\mu \ll 1/(K \log K) \quad (4.6)$$

ensures that no mutation occurs during the equilibration phase in the phenotypic space.

Consider as initial condition $n(0) = (n_{(g,p_1)}(0), \dots, n_{(g,p_\ell)}(0))$ a stable fixed point, $\bar{\mathbf{n}}$, of the following system:

$$\dot{\mathbf{n}}_{(g,p_i)} = \mathbf{n}_{(g,p_i)} \left(b_i - d_i - \sum_{j=1}^{\ell} c_{ij} \mathbf{n}_{(g,p_j)} - \sum_{j=1}^{\ell} s_{ij} \right) + \sum_{j=1}^{\ell} s_{ji} \mathbf{n}_{(g,p_j)}, \quad i = 1, \dots, \ell. \quad (4.7)$$

We write for simplicity $b_i = b(p_i)$, $d_i = d(p_i)$, $c_{ij} = c(p_i, p_j)$, $s_{ij} = s_g(p_i, p_j)$, and later $b'_i = b(p'_i)$, $d'_i = d(p'_i)$, $c'_{ij} = c(p'_i, p'_j)$, $\tilde{c}_{ij} = c(p_i, p'_j)$, $s'_{ij} = s_{g'}(p'_i, p'_j)$.

We want to analyse whether a single mutant appearing with a new genotype g' (and one of its possible phenotypes p'_i), has a positive probability to give rise to a population of size of order K . Using the same arguments as Champagnat et al. [8, 12], it is easy to show that as long as the mutant population has less than ϵK individuals (with $\epsilon \ll 1$), the mutant population $(g', p'_1), \dots, (g', p'_k)$ is well approximated by a k -type branching process, where each individual undergoes binary branching, death, or switch to another phenotype with the following rates:

$$\left. \begin{array}{ll} p'_i \rightarrow p'_i p'_i & \text{with rate } b'_i \\ p'_i \rightarrow \emptyset & \text{with rate } d'_i + \sum_{l=1}^{\ell} \tilde{c}_{il} \bar{\mathbf{n}}_l \\ p'_i \rightarrow p'_j & \text{with rate } s'_{ij} \end{array} \right\} \quad \text{for } i, j \in \{1, \dots, k\}. \quad (4.8)$$

where $(\bar{\mathbf{n}}_1, \dots, \bar{\mathbf{n}}_\ell)$ denotes the fixed point of (4.7). We will assume that the switch rates s'_{ij} are the transition rates of a Markov chain on $\{1, \dots, k\}$ which has a single recurrent class. The simplest example is the case where $s'_{ij} > 0$, for all $i, j \in \{1, \dots, k\}$.

Multi-type branching processes have been analysed by Kesten and Stigum [27, 26, 28] and Atreya and Ney [2]. Their behavior are classified in terms of the matrix A , given by

$$A = \begin{pmatrix} f_1 & s'_{12} & \dots & s'_{1k} \\ s'_{21} & f_2 & & \vdots \\ \vdots & & \ddots & \\ s'_{k1} & \dots & & f_k \end{pmatrix}, \quad (4.9)$$

where

$$f_i := b'_i - d'_i - \sum_{l=1}^{\ell} \tilde{c}_{il} \cdot \bar{\mathbf{n}}_l - \sum_{j=1}^k s'_{ij}, \quad i = 1, \dots, k. \quad (4.10)$$

Note that f_i would be the invasion fitness of phenotype i if there was no switch back from the other phenotypes to i (or if all switched cells would be killed). It is well-known that the multi-type process is super-critical, if and only if the largest eigenvalue, $\lambda_1 = \lambda_1(A)$, of the matrix A is strictly positive, meaning that if $\lambda_1 > 0$, the mutant population will grow with positive probability to any desired population size before dying out. Thus $\lambda_1(A)$ is the appropriate generalization of the invasion fitness:

$$F(g', g) := \lambda_1(A). \quad (4.11)$$

This notion can easily be generalised to the case when the initial condition is the equilibrium population of several coexisting genotypes. Note that this notion of invasion fitness of course reduces to the standard one of [8] if there is only one mutant phenotype. This settles the first step of our analysis, which is the invasion of the mutant.

Towards a generalised PES. In fact, one can say more about how the mutant population grows. Write $Z_j^{(i)}(t)$ for the number of individuals of phenotype p_j existing at time t for this branching process when the first mutant is of phenotype p_i . Then, for $i, j \leq k$,

$$\mathbb{E}(Z_j^{(i)}(t)) = [M(t)]_{i,j} \quad (4.12)$$

where $M(t)$ is the $k \times k$ -matrix

$$M(t) = \exp(At). \quad (4.13)$$

Assume that the largest eigenvalue $\lambda_1(A)$ is simple and strictly positive. Let v and u be the left and right eigenvectors of A associated to λ_1 , normalised such that $u \cdot v = 1$ and $u \cdot \mathbf{1} = 1$. The extinction probability vector $q = (q_1, \dots, q_k)$ where $q_i = \mathbb{P}(Z^{(i)}(t) = 0 \text{ for some } t)$ is the unique solution of the system of equations:

$$d'_i + \sum_{l=1}^{\ell} \tilde{c}_{il} \bar{n}_l + b'_i q_i^2 + \sum_{j=1}^k s'_{ij} q_j = q_i, \quad i = 1, \dots, k \quad (4.14)$$

which has in general no analytical solution. Then the following limit theorem holds [27]:

$$\lim_{t \rightarrow \infty} \left(Z_1^{(i)}(t), \dots, Z_k^{(i)}(t) \right) e^{-\lambda_1 t} = W_i \cdot (v_1, \dots, v_k) \quad \text{a.s.} \quad (4.15)$$

where $(W_i)_{i=1, \dots, k}$ is random vector with non-negative entries such that

$$\mathbb{P}(W_i = 0) = q_i \quad \text{and} \quad \mathbb{E}(W_i) = u_i. \quad (4.16)$$

In particular, conditionally on survival, the phenotypic distribution of the mutant populations converges almost surely to a deterministic quantity, which moreover does not depend on the phenotype of the initial mutant, namely

$$\lim_{t \rightarrow \infty} \frac{Z_{j'}^{(i)}(t)}{\sum_{j=1}^k Z_j^{(i)}(t)} = \frac{v_{j'}}{\sum_{j=1}^k v_j}, \quad \forall i, j' = 1, \dots, k. \quad (4.17)$$

For us, this implies the important fact that the phenotypic structure of the mutant population once it reaches the level $\varepsilon K > 0$ is almost deterministic. Then, conditionally on survival, (4.15) implies that the time $\tau_{\varepsilon K}$ until the total mutant population reached εK is of order $\log(K)$. Moreover, the proportions of the k types of phenotypes converge to deterministic quantities given above,

$$\frac{1}{K} (Z_1(\tau_{\varepsilon K}), \dots, Z_k(\tau_{\varepsilon K})) \rightarrow \left(\frac{\varepsilon v_1}{\sum_{j=1}^k v_j}, \dots, \frac{\varepsilon v_k}{\sum_{j=1}^k v_j} \right), \quad \text{in distribution, as } K \rightarrow \infty. \quad (4.18)$$

Once the mutant population has reached the level εK , the behavior of the process can be approximated by the solution of the deterministic system:

$$\begin{cases} \dot{\mathbf{n}}_{(g,p_i)} = \mathbf{n}_{(g,p_i)} \left(b_i - d_i - \sum_{j=1}^{\ell} s_{ij} - \sum_{j=1}^{\ell} c_{ij} \mathbf{n}_{(g,p_j)} - \sum_{j=1}^k \tilde{c}_{ij} \mathbf{n}_{(g',p'_j)} \right) + \sum_{j=1}^{\ell} s_{ji} \mathbf{n}_{(g,p_j)}, \\ \dot{\mathbf{n}}_{(g',p'_i)} = \mathbf{n}_{(g',p'_i)} \left(b'_i - d'_i - \sum_{j=1}^k s'_{ij} - \sum_{j=1}^k c'_{ij} \mathbf{n}_{(g',p'_j)} - \sum_{j=1}^{\ell} \tilde{c}_{ij} \mathbf{n}_{(g,p_j)} \right) + \sum_{j=1}^k s'_{ji} \mathbf{n}_{(g',p'_j)}, \end{cases} \quad (4.19)$$

(where i runs from 1 to ℓ in the first line and from 1 to k in the second one) with initial conditions in a small neighborhood of

$$(\mathbf{n}_{(g,p_1)}(0), \dots, \mathbf{n}_{(g,p_{\ell})}(0), \mathbf{n}_{(g',p'_1)}(0), \dots, \mathbf{n}_{(g',p'_k)}(0)) = \left(\bar{\mathbf{n}}_1, \dots, \bar{\mathbf{n}}_{\ell}, \frac{\varepsilon v_1}{\sum_{j=1}^k v_j}, \dots, \frac{\varepsilon v_k}{\sum_{j=1}^k v_j} \right). \quad (4.20)$$

If the system (4.19) is such that a neighborhood of (4.20) is attracted to the same fixed point, we are in the same situation as in Champagnat and Méléard [12] and get the first step in the Polymorphic Evolution Sequence.

Observe that in the case when the system of equations (4.19) has multiple attractors, and different points near (4.20) lie in different basins of attraction, then for finite K , the choice of attractor the system approaches may be random.

The characterization of the asymptotic behavior of the system (4.19) is needed to describe the final state of our stochastic process. This is in general a very difficult and complex problem, which is not doable analytically and will require numerical analysis.

Figure 10 (left) shows an example of the case discussed above with the following parameters:

$$\begin{array}{llll}
 b_0 = 5 & b_1 = 6 & b_2 = 6 & s_{12} = 2 \\
 d_0 = 0 & d_1 = 0 & d_2 = 0 & s_{21} = 2 \\
 c_{00} = 1 & c_{10} = 1 & c_{20} = 1 & \\
 c_{01} = 1 & c_{11} = 1 & c_{21} = 0 & (4.21) \\
 c_{02} = 0 & c_{12} = 0 & c_{22} = 1 & \\
 \mathbf{n}_{(g,p)}(0) = 5 & \mathbf{n}_{(g',p'_1)}(0) = 1/200 & \mathbf{n}_{(g',p'_2)}(0) = 0 & K = 200
 \end{array}$$

For these parameters f_1 and f_2 as defined in (4.10) are negative, but, due to the cooperation of the two phenotypes, the fitness of the genotype is positive and it invades with positive probability as indicated by the definition (4.11). In other words, each of the phenotypes is subcritical on its own, and supercriticality of the genotype is a consequence of the switch between the two phenotypes. Moreover, both phenotypes appear on a macroscopic level.

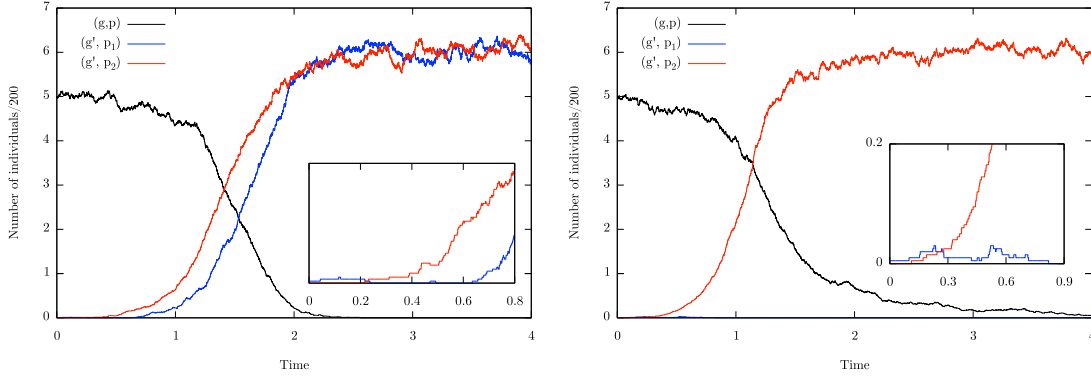


Fig. 10: (Left) An example where $f_1, f_2 < 0$, but $F(g, g') > 0$: $s_{12} = s_{21} = 2$, $f_1 = f_2 = -1$, $F(g', g) = \lambda_1 = 1$;
(Right) An example with unidirectional switch from a sub- to a supercritical phenotype : $s_{12} = 0$, $s_{21} = 2$, $f_1 = 1$, $f_2 = -1$, $F(g', g) = f_1 = 1$.

On Figure 10 (right) is an example with a vanishing switch rate, with the following parameters:

$$\begin{array}{llll}
 b_0 = 5 & b_1 = 6 & b_2 = 6 & s_{12} = 0 \\
 d_0 = 0 & d_1 = 0 & d_2 = 0 & s_{21} = 2 \\
 c_{00} = 1 & c_{10} = 1 & c_{20} = 1 & \\
 c_{01} = 1 & c_{11} = 1 & c_{21} = 0 & (4.22) \\
 c_{02} = 0 & c_{12} = 0 & c_{22} = 1 & \\
 \mathbf{n}_{(g,p)}(0) = 5 & \mathbf{n}_{(g',p'_1)}(0) = 0 & \mathbf{n}_{(g',p'_2)}(0) = 1/200 & K = 200
 \end{array}$$

In this case, p'_2 can switch to p'_1 but not the other way around, and we have $f_2 < 0$ and $f_1 > 0$ according to definition (4.10). If the first mutant is of phenotype p'_1 , the mutant population grows with rate f_1 , and if the first mutant is of phenotype p'_2 , which is sub-critical on its own, it switches with positive probability to the supercritical phenotype p'_1 . The global fitness of the genotype g' is positive and equal to f_1 .

4.3 The effect of birth-reducing competition on mutation events

In the previous section we considered the probability of invasion of a mutant when the resident population is at an equilibrium given by a fixed point. In the context of immunotherapy, there are phases when populations shrink and regrow due to treatment and relapse phenomena. In the medical literature, there are frequent allusions to the possibility that such growth cycles may induce fixation of a "super-resistant mutant", see e.g. [19, 25, 21]. It is an important question to understand whether and under what circumstances such effects may happen. Here we show a particular example where the appearance of a mutant genotype may indeed be enhanced in the relapse phase under treatment.

The effect is particularly prominent in the case where the competition between tumor cells is mainly acting through a reduction of birth rates, *i.e.* when the effect of the term in the third line of (2.13) (which we call birth-reducing competition) dominates the enhancement of death rates in the second line. In particular, in a large population at equilibrium, there may be fewer births and hence mutations, than in a smaller population growing towards its equilibrium size.

Let us explain this in more detail and discuss how the birth-reducing competition can have a crucial effect on the mutation timescale. For the sake of simplicity we consider an example where the switching rates are set to 0. Consider a melanoma population (g, p) which is able to mutate to a fitter type of melanoma (g', p') . We allow for one T-cell population attacking the resident melanoma population since this is the simplest scenario where the effect of therapy in this context can be explained. As the presence of TNF- α only influences the switch between phenotypes, it does not play any role in this example and we can set the corresponding parameters (ℓ_w and $d(w)$) to zero without loss of generality. If $\mu_g = \mu_g(K) \rightarrow 0$ as $K \rightarrow \infty$ the limiting deterministic system is given by:

$$\begin{cases} \dot{\mathbf{n}}_{(g,p)} &= \mathbf{n}_{(g,p)} (b(p) - d(p) - c_b(p, p)\mathbf{n}_{(g,p)} - c_b(p, p')\mathbf{n}_{(g',p')} - t(z, p)\mathbf{n}_z) \\ \dot{\mathbf{n}}_{(g',p')} &= \mathbf{n}_{(g',p')} (b(p') - d(p') - c_b(p', p')\mathbf{n}_{(g',p')} - c_b(p', p)\mathbf{n}_{(g,p)}) \\ \dot{\mathbf{n}}_z &= (b(z, p)\mathbf{n}_{(g,p)} - d(z))\mathbf{n}_z \end{cases} \quad (4.23)$$

Note that the mutation term does not appear in the deterministic system and that the difference between birth-reducing competition and usual competition is not visible. The effects we are looking for are intrinsically stochastic and happen on time-scales that diverge with K .

The interesting choice for the mutation rates is $K\mu_g(K) \rightarrow \alpha > 0$ as $K \rightarrow \infty$. In this case, there will be a number of mutations of order one while the population grows by $O(K)$ individuals. For lower mutation rates, no mutant can be expected before a population reaches its equilibrium, while for higher mutation rates the proliferation of mutants is unrealistically fast.

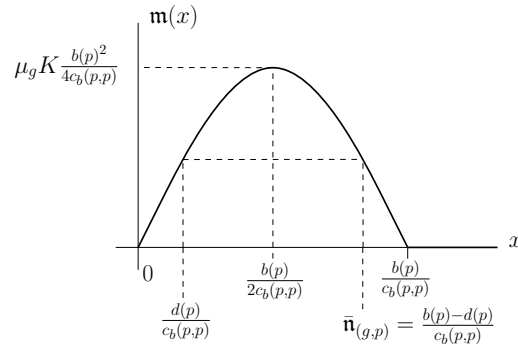


Fig. 11: Shape of the initial total mutation rate of the population (g, p) .

If the competition is only of birth-reducing type, then the total mutation rate of the population of type (g, p) at time t is

$$\mathbf{m}(\nu_t^K(g, p)) := \mu_g [b(p) - c_b(p, p)\nu_t^K(g, p)]_+ \nu_t^K(g, p)K. \quad (4.24)$$

This is a positive and concave function of $\nu_t^K(g, p)$ on the interval $[0, b(p)/c_b(p, p)]$, see Figure 11. If the population is at equilibrium (without or before therapy), meaning $\nu_t^K(g, p) = \bar{n}_{(g,p)} = (b(p) - d(p))/c_b(p, p)$, then the time until a mutation occurs is approximately exponentially distributed with parameter equal to

$$\mu_g K \cdot (b(p) - c_b(p, p) \bar{n}_{(g,p)}) \bar{n}_{(g,p)} = \mu_g K \cdot d(p) \bar{n}_{(g,p)}. \quad (4.25)$$

If $d(p)$ is smaller than $b(p)/2$, then $\bar{n}_{(g,p)}$ is bigger than $b(p)/2c_b(p, p)$ and $m(\bar{n}_{(g,p)})$ is not maximal. Smaller populations, more precisely in between $d(p)/c_b(p, p)$ and $\bar{n}_{(g,p)}$, have a higher total mutation rate.

This situation can happen during a T-cell therapy. Indeed, the introduction of T-cells in the system lowers the average population of melanoma (usually by making it undergo a damped cycle), and there exist parameters such that the mutation rate of (g, p) is larger during the treatment, for the reason explained above.

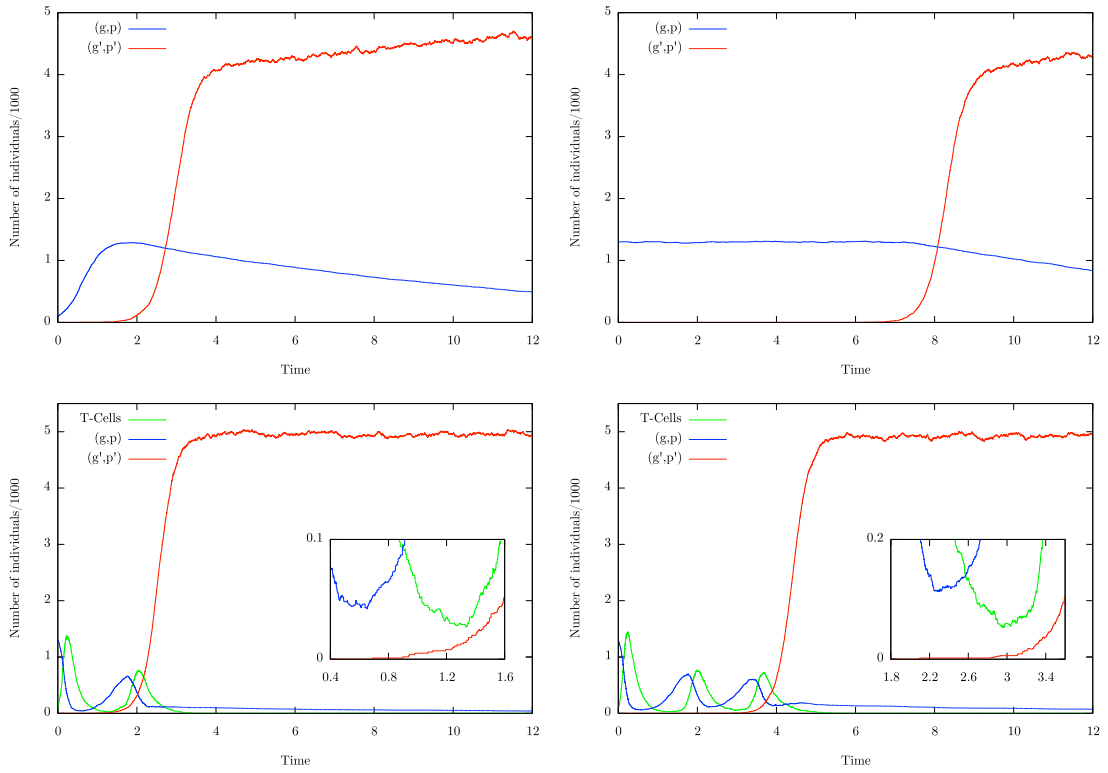


Fig. 12: Example of earlier mutation induced by therapy, with parameters given by (4.26). (Top Left) Starting with a small population without therapy; (Top Right) Starting with a population at its equilibrium without therapy; (Bottom) Starting with a population at its equilibrium with therapy (2 examples with same parameters).

Figure 12 illustrates this situation with the following parameters (all the other ones described in Section 2.1 being set to 0):

$$\begin{array}{llll}
 b(p) = 4 & b(p') = 6 & b(z, p) = 20 & m((g, p), (g', p')) = 1 \\
 d(p) = 0.1 & d(p') = 1 & t(z, p) = 10 & \mu_g = 10^{-3} \\
 c_b(p, p) = 3 & c_b(p', p) = 0.8 & d(z) = 6 & K = 10^3 \\
 c_b(p, p') = 0.8 & c_b(p', p') = 1 & & \\
 \mathbf{n}_{(g,p)}(0) = 1.3 & \mathbf{n}_{(g',p')}(0) = 0 & \mathbf{n}_z(0) = 0 \text{ or } 0.1 &
 \end{array} \quad (4.26)$$

On the top-left of Figure 12 the effect of birth-reducing competition on mutations in small populations is shown; on the top-right of the figure is a realization of the case without therapy starting at the equilibrium of the melanoma population, with average mutation time equal to 7.7 (computed as $1/m(\bar{n}_{(g,p)})$), and on the bottom are realizations of the case with T-cell therapy, with average mutation time smaller than in the equilibrium case.

Note that this example provides an interesting situation of interplay between therapy and mutation. By lowering the melanoma population, the T-cell therapy actually increases the probability for it to mutate to a potentially fitter and pathogenic genotype, which is not affected by the T-cells.

5 Prediction of the efficacy of immunotherapeutic methods

5.1 Therapy with T-cells of one or two specificities with biologically reasonable parameters

The parameters in Subsections 4.1.1 and 4.1.2 were chosen ad hoc to give a clear picture of the influence of randomness and the possible behaviour of the system. Since we developed the model on the basis of the observations made in [30], let us show that experimental observations can be matched by the model for physiologically reasonable parameters. Some parameters can be estimated from the experimental data. Recall that the subject of [30] is to investigate the behaviour of melanoma under T-cell therapy in mice. Without therapy the tumor undergoes only natural birth, death and switch events.

- *Estimation of birth and death rates:* We assume that the number of cells in the tumor is described by

$$N_t \approx N_0 \exp(rt), \quad (5.1)$$

where N_t denotes the number of cells at time t , N_0 the initial population size and r the overall growth rate. Note that the estimate of the growth rate is independent of the initial value. Figure 1a in [30] shows that the tumor needs roughly 50 days (without therapy) to grow from 2mm diameter to 10mm diameter. Since the structure of a melanoma is 3-dimensional this corresponds to $N_{50} = 125N_0$ which implies $r = 0.1$. Unfortunately, no data that allow to estimate the ratio of birth and death events are provided. As long as mutations are not considered this should not have a big impact and we chose $b = 0.12$ and $d = 0.02$ for the differentiated as well as the dedifferentiated cells, see Figure 15. Landsberg et al. observed that the growth kinetics appear to be the same for both cell types, compare to Supplementary Figure 11 in [30].

- *Estimation of the competition:* We assume that the competition has a very little effect here because the tumor grows exponentially in the observed time frame and does not come close to its equilibrium. We chose the competition between melanoma cells of the same type as $c(x, x) = c(y, y) = 0.00005$ and between different types of melanoma cells as $c(x, y) = c(y, x) = 0.00002$. The values are not set to 0 since the melanoma can grow only up to a finite size.
- *Estimation of the switch parameters:* We can now estimate (roughly) the switching parameters by using the data of Supplementary Figure 9e. In this experiment where cell division is inhibited, we can set $b = 0$. Furthermore, the amount of TNF- α is constant and we set here $n_w = 2$. Thus, the dynamics of the melanoma populations is described by

$$\begin{cases} \dot{n}_x = n_x(-d(x) - c(x, x)n_x - c(x, y)n_y - 2s_w(x, y) - s(x, y)) + s(y, x)n_y \\ \dot{n}_y = n_y(-d(y) - c(y, y)n_y - c(y, x)n_x - s(y, x)) + (2s_w(x, y) + s(x, y))n_x \end{cases} \quad (5.2)$$

At the beginning of their observations the switch is very slow and speeds up after the first 24 hours. We assume that there is a delay until the reaction really starts and thus we chose the proportions at day 1 ($n_x = 0.81$ and $n_y = 0.19$) as initial data and chose switching parameters such that roughly the concentrations at day 2 ($n_x = 0.45$ and $n_y = 0.54$) and 3 ($n_x = 0.24$ and $n_y = 0.72$) are reached as shown in Figure 13. Thereby we obtain $s(x, y) = 0.0008$, $s(y, x) = 0.065$ and $s_w(x, y) = 0.33$. Note that the experiments we refer to provide only in vitro data and it is not clear if the in vivo situation is similar.

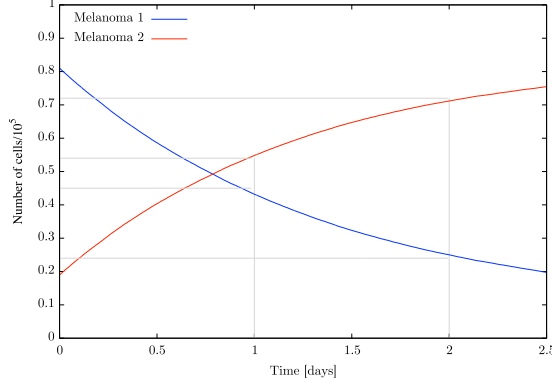


Fig. 13: Switch in the in vitro experiments for inhibited cell division and constant concentration of TNF- α . The grey lines indicate the experimental data.

- *Estimation of parameters concerning T-cells:* It remains to characterise the T-cells. Their natural birth rate is set to 0 since they are transferred by adoptive cell transfer and not produced by the mice themselves and do not proliferate in absence of targets. We assume that they have a relatively high birth rate depending on the amount of cancer cells present, $b(z_x, x) = b(z_y, y) = 2$ and produce one TNF- α molecule when they divide, $\ell_w(z_x) = \ell_w(z_y) = 1$. Furthermore, we assume that they can kill 4.5 cancer cells per hour, $t(z_x, x) = t(z_y, y) = 108$. The rate of death for the T-cell population is chosen as $d(z_x) = d(z_y) = 0.12$. These parameters were chosen such that the qualitative behaviour of the tumor was recovered as shown in Figure 15. We chose the same parameters for the second T-cell type as for the first one because there are no data concerning the second T-cell type.
- *Choice of starting values and the scale K :* We set $K = 10^5$, the initial value for the differentiated melanoma cell population to 1 and to 0 for the population of dedifferentiated melanoma cells. The ratio of differentiated and dedifferentiated cells is not known for small tumors which do not result from cell transfer of cells of in vitro cell lines. The initial value of the T-cell population is set to 0.02.

To sum up, biological rates (per day) and initial conditions (in 100 000 cells) are:

$$\begin{array}{llll}
 b(x) = 0.12 & b(y) = 0.12 & b(z_x, x) = 2 & \ell_w(z_x) = 1 \\
 d(x) = 0.02 & d(y) = 0.02 & t(z_x, x) = 108 & d(w) = 0.2 \\
 c(x, x) = 5 \cdot 10^{-5} & c(x, y) = 2 \cdot 10^{-5} & d(z_x) = 0.12 & s_w(x, y) = 0.33 \\
 c(y, x) = 2 \cdot 10^{-5} & c(y, y) = 5 \cdot 10^{-5} & & \\
 s(x, y) = 0.0008 & s(y, x) = 0.065 & & \\
 n_x(0) = 1 & n_y(0) = 0 & n_{z_x}(0) = 0.02 & K = 10^5
 \end{array} \tag{5.3}$$

The therapy with one type of T-cells pushes the tumor down to a microscopic level for 50 to 60 days as shown in Figure 14. The decrease is fast but at the order of days (not hours). In the simulations two scenarios can occur: first, the relapse consists mainly of differentiated melanoma cells and the melanoma reaches its original size again after 90 days. This is the case when the T-cells died out (shown on the left of Figure 14). Second, the relapse consists to a high amount of dedifferentiated cells. This is the case when the T-cells survived the phase when the tumor was small and become active again and kill differentiated cancer cells (shown on the right of Figure 14). In this case the tumor reaches its original size again after roughly 190 days. On the left of Figure 15 the experimental data of [30] are shown. On the right of the figure the results of our simulations for parameters as indicated in Equations (5.3) are shown. Each line corresponds to the total size of a tumor measured in diameter and tracked over time. The lines for the experimental

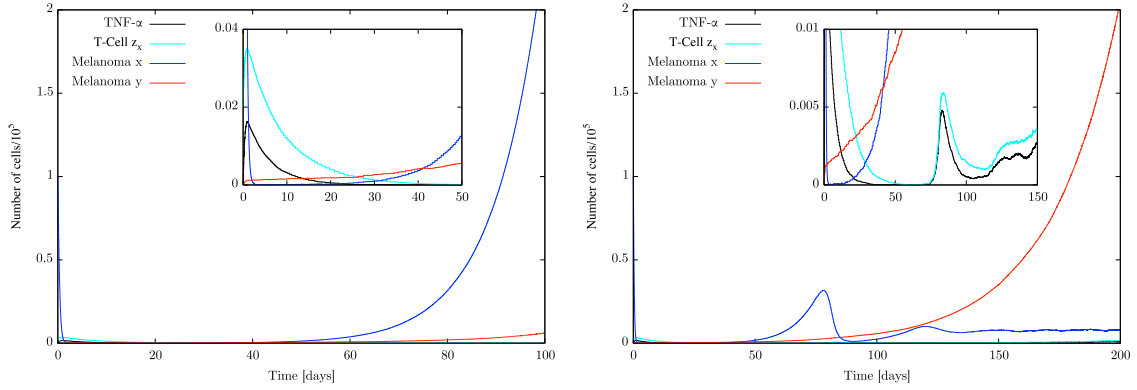


Fig. 14: Two different relapse behaviour

data marked by ACT correspond to the cases in the simulations where the active T-cells died out. In the experiments there might be T-cells present but they lost their function and cannot kill the differentiated melanoma cells. They can be restimulated and become active again which is marked as ACT+Re. This case corresponds to simulations where the population of active T-cells survived. The timescale for the experimental data start at day 0 of DMBA, i.e. day 0 of tumor initiation. We do not model this phase and thus the simulated curves start at the tumor measurements. Note that labelling of time axis is the same in both figures. One can see that the experimental findings are met very well by the simulations.

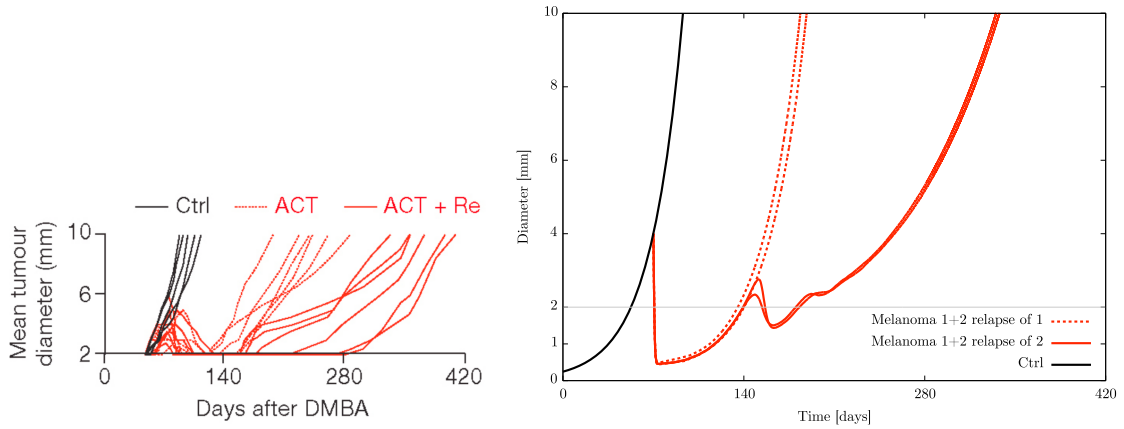


Fig. 15: Comparison of experimental (Left) and simulated (Right) data.

As there are no data for the case of two T-cells, numerical simulations of such a therapy strategy should be seen as predictions. For the new T-cell population we chose the same parameters as for the first population, just the target is different.

The additional parameters are:

$$t(z_y, y) = 108 \quad \ell_w(z_y) = 1 \quad b(z_y, y) = 2 \quad d(z_y) = 0.12 \quad \mathbf{n}_{z_y}(0) = 0.02 \quad (5.4)$$

With the above deduced parameters and the guess for the parameters for a second type of T-cell the therapy approach seems to be very promising: almost all simulations have shown a cure for these parameters as shown on the left of Figure 16. Only very few times a relapse occurs as shown on the right of Figure 16. Nevertheless, it was pointed out in subsection 4.1.2 that the behaviour of the system with two types of T-cells can be very complicated. It depends strongly on the choice of

certain parameters, e.g. on the switching parameters. In order to give a reliable prediction we need data to obtain safer estimates for the most important parameters, which seem to be the switching and killing rates as well as the initial values at the beginning of therapy. Moreover, it is of course possible that in reality something happens which is not possible to predict with this model, e.g. an additional escape strategy of the dedifferentiated melanoma cells could be observed.

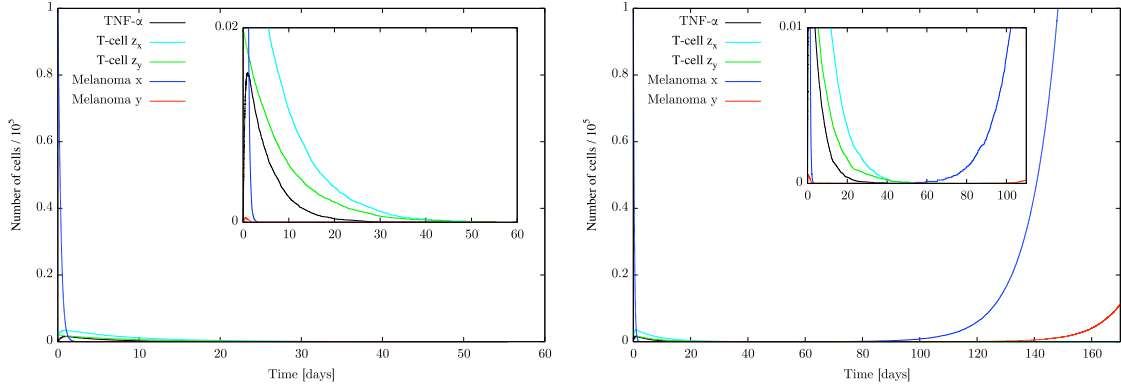


Fig. 16: Two possible behaviours for therapy with two different types of T-cells

5.2 Initial values

Also the initial values play an important role for the success of a therapy. When we consider the case of therapy with T-cells of one specificity increasing the initial amount of T-cells has the following effect: the melanoma cells are killed faster, the minimum of the population of differentiated melanoma cells reaches a lower minimum and as a consequence also the T-cells pass through a lower and broader minimum in the deterministic system.

The probability that the T-cells die out increases and a differentiated relapse is observed more often than in the case of a smaller initial T-cell population. Moreover, the broadening of the minima causes a “delay” and both kind of relapses (mainly differentiated or dedifferentiated one) appear later compared to the lower initial value of T-cells. But since the T-cells die out more often the tumor reaches its original size on average earlier. For the parameters of subsection 5.1, taking an initial value 10 times as large as done in the subsection can cause a cure very rarely. If it is set to half the number of cancer cells a cure can be observed more often. But such a high amount of T-cells is probably infeasible.

5.3 Therapy-induced early mutation

Therapy can also have an effect on the probability for a mutation to appear and the expected time until mutations appear as explained in subsection 4.3. Therapy for a tumor which stays in an equilibrium under influence of birth-reducing competition can increase proliferation and thus mutation rates in comparison to an untreated tumor. In this case the treatment could lead to earlier mutations and thus earlier aggressive tumor variants which is not desirable.

References

1. T. Antal and P. Krapivsky. Exact solution of a two-type branching process: models of tumor progression. *J. Stat. Mech. Theory Exp.*, 2011(08):P08018, 2011.
2. K. B. Athreya and P. E. Ney. *Branching processes*. Dover Publications, Inc., Mineola, NY, 2004. Reprint of the 1972 original [Springer, New York; MR0373040].
3. M. Baar, A. Bovier, and N. Champagnat. From stochastic, individual-based models to the canonical equation of adaptive dynamics - in one step. In preparation, 2015.
4. B. Bolker and S. W. Pacala. Using moment equations to understand stochastically driven spatial pattern formation in ecological systems. *Theoret. Population Biol.*, 52(3):179 – 197, 1997.
5. B. M. Bolker and S. W. Pacala. Spatial moment equations for plant competition: understanding spatial strategies and the advantages of short dispersal. *The American Naturalist*, 153(6):575–602, 1999.
6. A. Bovier and S.-D. Wang. Trait substitution trees on two time scales analysis. *Markov Process. Related Fields*, 19(4):607–642, 2013.
7. I. Bozic, T. Antal, H. Ohtsuki, H. Carter, D. Kim, S. Chen, R. Karchin, K. W. Kinzler, B. Vogelstein, and M. A. Nowak. Accumulation of driver and passenger mutations during tumor progression. *Proc. Nat. Acad. Sci. USA*, 107(43):18545–18550, 2010, <http://www.pnas.org/content/107/43/18545.full.pdf+html>.
8. N. Champagnat. A microscopic interpretation for adaptive dynamics trait substitution sequence models. *Stochastic Process. Appl.*, 116(8):1127–1160, 2006.
9. N. Champagnat, R. Ferrière, and G. Ben Arous. The canonical equation of adaptive dynamics: A mathematical view. *Selection*, 2:73–83, 2001.
10. N. Champagnat, R. Ferrière, and S. Méléard. From individual stochastic processes to macroscopic models in adaptive evolution. *Stoch. Models*, 24(suppl. 1):2–44, 2008.
11. N. Champagnat, P.-E. Jabin, and S. Méléard. Adaptation in a stochastic multi-resources chemostat model. *J. Math. Pures Appl. (9)*, 101(6):755–788, 2014.
12. N. Champagnat and S. Méléard. Polymorphic evolution sequence and evolutionary branching. *Probab. Theory Related Fields*, 151(1-2):45–94, 2011.
13. A. L. Correia and M. J. Bissell. The tumor microenvironment is a dominant force in multidrug resistance. *Drug Resistance Updates*, 15(1):39–49, 2012.
14. M. Costa, C. Hauzy, N. Loeuille, and S. Méléard. Stochastic eco-evolutionary model of a prey-predator community. July 2014, arXiv:1407.3069.
15. Dieckmann and Law. Moment approximations of individual-based models. In U. Dieckmann, R. Law, and J. A. J. Metz, editors, *The geometry of ecological interactions: simplifying spatial complexity*, pages 252–270. Cambridge University Press, 2000.
16. R. Eftimie, J. Bramson, and D. Earn. Interactions between the immune system and cancer: A brief review of non-spatial mathematical models. *Bulletin of Mathematical Biology*, 73(1):2–32, 2011.
17. S. N. Ethier and T. G. Kurtz. *Markov processes*. Wiley Series in Probability and Mathematical Statistics: Probability and Mathematical Statistics. John Wiley & Sons, Inc., New York, 1986.
18. N. Fournier and S. Méléard. A microscopic probabilistic description of a locally regulated population and macroscopic approximations. *Ann. Appl. Probab.*, 14(4):1880–1919, 2004.
19. S. A. Frank and M. R. Rosner. Nonheritable cellular variability accelerates the evolutionary processes of cancer. *PLoS Biol.*, 10(4):e1001296, 2012.
20. R. J. Gillies, D. Verduzco, and R. A. Gatenby. Evolutionary dynamics of carcinogenesis and why targeted therapy does not work. *Nat. Rev. Cancer*, 12(7):487–493, 2012.
21. M. Greaves and C. C. Maley. Clonal evolution in cancer. *Nat Rev*, 481:306–313, 2012.
22. P. B. Gupta, C. M. Fillmore, G. Jiang, S. D. Shapira, K. Tao, C. Kuperwasser, and E. S. Lander. Stochastic state transitions give rise to phenotypic equilibrium in populations of cancer cells. *Cell*, 146(4):633–644, 2011.
23. D. Hanahan and R. A. Weinberg. Hallmarks of cancer: the next generation. *Cell*, 144(5):646–674, 2011.
24. M. Hözl, A. Bovier, and T. Tüting. Plasticity of tumour and immune cells: a source of heterogeneity and a cause for therapy resistance? *Nat. Rev. Cancer*, 13(5):365–376, 05 2013.
25. G. R. J., D. Verduzco, and R. A. Gatenby. Evolutionary dynamics of carcinogenesis and why targeted therapy does not work. *Nat. Rev. Cancer*, 12(7):487–93, 2012.
26. H. Kesten and B. P. Stigum. Additional limit theorems for indecomposable multidimensional Galton-Watson processes. *Ann. Math. Statist.*, 37:1463–1481, 1966.
27. H. Kesten and B. P. Stigum. A limit theorem for multidimensional Galton-Watson processes. *Ann. Math. Statist.*, 37:1211–1223, 1966.
28. H. Kesten and B. P. Stigum. Limit theorems for decomposable multi-dimensional Galton-Watson processes. *J. Math. Anal. Appl.*, 17:309–338, 1967.
29. V. Kuznetsov, I. Makalkin, M. Taylor, and A. Perelson. Nonlinear dynamics of immunogenic tumors: Parameter estimation and global bifurcation analysis. *Bull. Math. Biol.*, 56(2):295–321, 1994.
30. J. Landsberg, J. Kohlmeyer, M. Renn, T. Bald, M. Rogava, M. Cron, M. Fatho, V. Lennerz, T. Wölfel, M. Hölzel, and T. Tüting. Melanomas resist t-cell therapy through inflammation-induced reversible dedifferentiation. *Nature*, 490(7420):412–416, 10 2012.
31. A. Marusyk, V. Almendro, and K. Polyak. Intra-tumour heterogeneity: a looking glass for cancer? *Nat. Rev. Cancer*, 12(5):323–334, 2012.
32. J. A. J. Metz, S. A. H. Geritz, G. Meszéna, F. J. A. Jacobs, and J. S. van Heerwaarden. Adaptive dynamics, a geometrical study of the consequences of nearly faithful reproduction. In *Stochastic and spatial structures of dynamical systems (Amsterdam, 1995)*, Konink. Nederl. Akad. Wetensch. Verh. Afd. Natuurk. Eerste Reeks, 45, pages 183–231. North-Holland, Amsterdam, 1996.